A Framework for Transceiver Designs for Multi-Hop Communications with Covariance Shaping Constraints

Chengwen Xing, Feifei Gao, and Yiqing Zhou

arXiv:1411.4249v4 [cs.IT] 11 Dec 2014

Abstract

For multiple-input multiple-output (MIMO) transceiver designs, sum power constraint is an elegant and ideal model. When various practical limitations are taken into account e.g., peak power constraints, per-antenna power constraints, etc., covariance shaping constraints will act as an effective and reasonable model. In this paper, we develop a framework for transceiver designs for multi-hop communications under covariance shaping constraints. Particularly, we focus on multi-hop amplify-and-forward (AF) MIMO relaying communications which are recognized as a key enabling technology for device-to-device (D2D) communications for next generation wireless systems such as 5G. The proposed framework includes a broad range of various linear and nonlinear transceiver designs as its special cases. It reveals an interesting fact that the relaying operation in each hop can be understood as a matrix version weighting operation. Furthermore, the nonlinear operations of Tomolision-Harashima Precoding (THP) and Decision Feedback Equalizer (DFE) also belong to the category of this kind of matrix version weighting operation. Furthermore, for both the cases with only pure shaping constraints or joint power constraints, the closed-form optimal solutions have been derived. At the end of this paper, the performance of the various designs is assessed by simulations.

Index Terms

Amplify-and-forward MIMO relaying, joint power constraints, shaping constraints.

C. Xing is with the School of Information and Electronics, Beijing Institute of Technology, Beijing, China (E-mail: chengwenxing@ieee.org).

F. Gao is with Tsinghua National Laboratory for Information Science and Technology, Tsinghua University, Beijing, China (E-mail: feifeigao@ieee.org)

Y. Zhou is with Institute of Computing Technology, Chinese Academy of Sciences, Beijing, China (E-mail: zhouyiqing@ict.ac.cn)

I. Introduction

Multi-hop relaying communications have attracted a lot of attention recently because of both its theoretical and practical importance [1]. From theoretical viewpoint, multi-hop relaying networks include some well-known systems such as dual-hop relaying and point-to-point communication systems as its special cases. Meanwhile, multi-hop relaying technique is a fundamental technique to enable device-to-device (D2D) communications [1], [2]. As it can effectively offload the traffic loads from overloaded macro base stations (BSs) to lightly loaded pico BSs or femto BSs or even small cell BSs, D2D communication technology is envisioned as a key enabling technology to realize high spectrum efficiency for next generation communication systems e.g., 5G wireless systems.

The relaying strategies at relays can be classified into various categories e.g., amplify-and-forward (AF), decode-and-forward (DF), compressed-and-forward (CF) and so on [3]. In general, each relaying strategy has its own advantages, and which one is the best is really a meaningless question without specific system settings. Due to implementation simplicity and security issue, AF strategies have gained lots of attention. With channel state information (CSI), transceiver designs can greatly improve system performance. Transceiver designs for AF MIMO relaying systems have been extensively studied in the literature [4]–[13].

When there are multiple data streams are transmitted simultaneously, it is hard to give a dominated performance metric which can be argued better than any another one. Generally speaking, there are various design criteria for transceiver designs for AF MIMO relaying networks. The most widely used criteria are capacity maximization [7], [8], [12] and data mean-square-error (MSE) minimization [9]–[12]. Capacity reflects how much information can be reliably transmitted, while MSE demonstrates how accurately the desired signals can be recovered at the destination. From the implementation point of view, transceivers designs can be classified into two main categories, i.e., linear transceiver designs and nonlinear transceiver designs. Linear transceiver designs can strick a balance between performance and complexity [12]. On the other hand, nonlinear transceiver designs can improve bit error rates (BERs) at the cost of high implementation complexity [14]. In the existing works, the nonlinear transceiver designs are usually referred to as the transceivers with Tomolision-Harashima Precoding (THP) at source or Decision Feedback Equalizer (DFE) at destination [14]. Furthermore, taking channel estimation

errors into account robust transceiver designs have also attracted lots of attention [15]–[20]. Following this logic, the transceiver designs for multi-hop AF MIMO relaying are investigated in [21]–[23], in which both linear and nonlinear transceiver designs are investigated with various performance metrics and even imperfect CSI

Most of the existing works mainly focus on the transceiver designs with simple and ideal sum power constraints. Unfortunately, there are many practical physical constraints in the practical transceiver designs. For example, as each antenna has its own power amplifier actually the dynamic range of each amplifier must not exceed a threshold and per-antenna power constraints may be more practical [24]. Moreover, sum power constraint is only a definition in the statistical average sense and thus there may be some outages for the specific power constraints at amplifiers. To relieve the outage effects, peak power constraint on the transmitted signal covariance matrix will be an effective model [24]–[26]. It is worth noting that l_p-norm power constraint can also be successfully approximated by joint power constraints consisting of shaping (maximum eigenvalue) and sum power constraints [27]. In order to take these constraints in account and still keep graceful closed-form solutions, covariance shaping constraints are usually exploited in the transceiver designs [24]–[27]. This kind of constraints can effectively mode practical constraints and avoid high complexity numerical computations in the transceiver deigns. In a nutshell, covariance shaping constraints are a kind of useful constraints limiting the transmit power in virtual spatial directions including spectral masks, peak power constraints, per-antenna power constraints and so on [24]–[26].

In this paper, we take a further step to investigate the transceiver designs for multi-hop cooperative networks under covariance shaping constraints. Both linear transceiver designs and nonlinear transceiver designs are taken into account. In particular, we investigate in depth the transceiver designs with pure shaping constraints and with joint power constraints comprising of sum power constraints and maximum eigenvalue constraints. The main contributions of our work are listed as follows.

(1). The proposed framework includes a wide range of transceiver designs as its special cases e.g., linear transceiver designs with additively Shur-convex/concave objective functions and nonlinear transceiver designs with multiplicatively Shur-convex/concave objective functions. The framework reveals a fact that for the various considered objective functions, in the nature they can always be unified into a multiple objective optimization problem. It is also shown by our

framework that the transceiver designs can be decomposed into a series of subproblems which only relate with their respective local CSI.

(2). Based on the proposed framework, an interesting and useful understanding of transceiver designs for multi-hop AF MIMO relaying is given. However for AF relaying strategy the noise at each relay will be amplified and forwarded to the next hop, this procedure can be understood as a matrix version weighting operation. Specifically, the AF relaying operation in any hop will act as a matrix weighting operation on the MSE of the remaining successive hops. It may be the reason why AF MIMO relaying looks complicated, but it usually enjoys elegant and simple optimal solutions just as point-to-point MIMO systems. In addition, for nonlinear transceiver designs, the nonlinear operations THP and DFE can also be understood as the same kind of matrix version weighting operation with different matrix version slope and intercept.

(3). For the transceiver designs under pure shaping constraints or joint power constraints, the explicit optimal structures of the optimal transceivers can be derived. On the one hand, the transceiver designs under pure shaping constraints have the explicit closed-form optimal solutions which are independent of the specific formulations of objective functions. On the other hand, for the transceiver designs under joint power constraints, based on the optimal structures the remaining variables are only a series of scalar variables that can be efficiently solved by a variant of water-filling solutions named cave water-filling solutions. These structures greatly simplify the practical designs and enable distributed implementation of the proposed algorithm.

The rest of this paper is organized as follows. In Section II, the system model is given and the unified transceiver design under covariance shaping constraints is formulated in Section III. After that, the considered optimization is simplified into a multi-objective optimization in Section IV. The optimal solutions for the transceiver designs with pure shaping constraints and joint power constraints are derived in Sections V and VI, respectively. The performance of the different designs is evaluated in Section VII. Finally, the lconclusions are drawn in Section VIII.

Notation: Throughout the whole paper, the following mathematical notations are used. Boldface lowercase letters denote vectors, and boldface uppercase letters denote matrices. The notation $\mathbf{Z}^{\mathrm{H}}$ denotes the Hermitian of the matrix $\mathbf{Z}$. The symbol $\mathrm{Tr}(\mathbf{Z})$ represents the trace of the matrix $\mathbf{Z}$. The symbol $\mathbf{I}_M$ denotes the $M \times M$ identity matrix, and $\mathbf{0}_{M,N}$ denotes the $M \times N$ all zero matrix. The notation $\mathbf{Z}^{1/2}$ is the Hermitian square root of the positive semidefinite matrix $\mathbf{Z}$, such that $\mathbf{Z}^{1/2}\mathbf{Z}^{1/2} = \mathbf{Z}$ and $\mathbf{Z}^{1/2}$ is also a Hermitian matrix. The symbol $\lambda_i(\mathbf{Z})$ represents the

i^{th} largest eigenvalue of $\mathbf{Z}$. For two Hermitian matrices, the equation $\mathbf{C} \succeq \mathbf{D}$ means that $\mathbf{C}-\mathbf{D}$ is a positive semi-definite matrix. The symbol $\mathbf{\Lambda} \searrow$ represents a rectangular diagonal matrix with nonincreasing diagonal elements.

II. System Model

In this paper, we are concerned with a multi-hop AF MIMO relaying network. As shown in Fig. 1, one source node with $N_{T,1}$ transmit antennas wants to communicate with a destination node with $N_{T,K}$ receive antennas through $K-1$ relay nodes. For the k^{th} relay, it has $N_{R,k}$ receive antennas and $N_{T,k+1}$ transmit antennas. In order to guarantee the transmitted data $\mathbf{s}$ can be recovered at the destination node, it is assumed that $N_{T,k}$ and $N_{R,k}$ are greater than or equal to N [9]. It is straightforward that the a dual-hop/two-hop AF MIMO relaying network is the special case with $K=2$.

At the source node, an $N \times 1$ data vector $\mathbf{a}$ with covariance matrix $\mathbf{R}_{\mathbf{a}} = \mathbb{E}\{\mathbf{a}\mathbf{a}^{\text{H}}\} = \sigma_{\mathbf{a}}^2\mathbf{I}_N$ is transmitted. It should be highlighted that in our work, both linear and nonlinear transmitters are taken into account. For nonlinear transmitters, before going through the precoder matrix $\mathbf{P}_1$ at the source, the vector $\mathbf{a}$ may be preprocessed first. As a result, the signal finally transmitted by the source is denoted by $\mathbf{x}_0$ instead of $\mathbf{a}$ and its specific formulas will be discussed later. The received signal $\mathbf{x}_1$ at the first relay is $\mathbf{x}_1 = \mathbf{H}_1\mathbf{P}_1\mathbf{x}_0 + \mathbf{n}_1$ where $\mathbf{H}_1$ is the MIMO channel matrix between the source and the first relay. In addition, $\mathbf{n}_1$ is the additive Gaussian noise vector at the first relay with mean zero and covariance matrix $\mathbf{R}_{n_1} = \sigma_{n_1}^2\mathbf{I}_{M_1}$.

The received signal $\mathbf{x}_1$ at the first relay node is first multiplied by a forwarding matrix $\mathbf{P}_2$ and then the resultant signal is transmitted to the second relay node. The received signal $\mathbf{x}_2$ at the second relay node is $\mathbf{x}_2 = \mathbf{H}_2\mathbf{P}_2\mathbf{x}_1 + \mathbf{n}_2$, where $\mathbf{H}_2$ is the MIMO channel matrix between the first and the second relay nodes. Additionally, $\mathbf{n}_2$ is the additive Gaussian noise vector at the second relay with mean zero and covariance matrix $\mathbf{R}_{n_2} = \sigma_{n_2}^2\mathbf{I}_{M_2}$. Similarly, the received signal at the k^{th} relay node can be written as

$$\mathbf{x}_k = \mathbf{H}_k\mathbf{P}_k\mathbf{x}_{k-1} + \mathbf{n}_k \tag{1}$$

where $\mathbf{H}_k$ is the channel for the k^{th} hop, and $\mathbf{n}_k$ is the additive Gaussian noise with mean zero and covariance matrix $\mathbf{R}_{n_k} = \sigma_{n_k}^2\mathbf{I}_{M_k}$. The received signal covariance matrix $\mathbf{R}_{\mathbf{x}_k}$ at the k^{th}

relay node satisfies the following recursive formula

$$\mathbf{R}_{\mathbf{x}_k} = \mathbf{H}_k \mathbf{P}_k \mathbf{R}_{\mathbf{x}_{k-1}} \mathbf{P}_k^{\mathrm{H}} \mathbf{H}_k^{\mathrm{H}} + \mathbf{R}_{n_k}. \tag{2}$$

The covariance matrix of the transmitted signal at the k^{th} node (including both source and relays) is $\mathbf{P}_k \mathbf{R}_{\mathbf{x}_{k-1}} \mathbf{P}_k^{\mathrm{H}}$ and in practice there are naturally several constraints on these covariance matrices. The most widely used constraint is the sum power constraint i.e., $\mathrm{Tr}(\mathbf{P}_k \mathbf{R}_{\mathbf{x}_{k-1}} \mathbf{P}_k^{\mathrm{H}}) \leq P_k$. In order to limit the transmit power in virtual spatial directions the covariance shaping constraint on the transmitted signal covariance matrix is formulated as

$$\mathbf{P}_k \mathbf{R}_{\mathbf{x}_{k-1}} \mathbf{P}_k^{\mathrm{H}} \preceq \mathbf{R}_{\mathbf{s}_k} \tag{3}$$

which includes the following constraints as its special cases [24].

• Peak power constraints:

Note that sum power constraints are defined in the sense of statistical average, but for each power amplifier the power budget limits are deterministic and independent with each other. To shrink the gap between practical phenomena and theoretical model, an effect way is to add peak power constraints [24]–[26], and therefore we have

$$\mathbf{P}_k \mathbf{R}_{\mathbf{x}_{k-1}} \mathbf{P}_k^{\mathrm{H}} \preceq \tau_{k,\max} \mathbf{I}. \tag{4}$$

• Independent Power Constraints Per Antenna:

A simple way to limit each diagonal element of the transmit covariance matrix i.e., $[\mathbf{P}_k \mathbf{R}_{\mathbf{x}_{k-1}} \mathbf{P}_k^{\mathrm{H}}]_{i,i} \leq P_{i,k}$ is to exploit the following constraint [24]

$$\mathbf{P}_k \mathbf{R}_{\mathbf{x}_{k-1}} \mathbf{P}_k^{\mathrm{H}} \preceq \mathrm{diag}\{\{p_{i,k}\}_{i=1}\}. \tag{5}$$

• Spectral mask:

For wire line systems e.g., digital subscriber line (DSL) spectral masks are exploited to guarantee spectral compatibility with different users that share the same cable simultaneously [24].

• Power constraint along a spatial direction:

Defining the direction by using unitary vector $\mathbf{u}$ the power in this direction equals $\mathbf{u}^{\mathrm{H}} \mathbf{R}_{\mathbf{s}_k} \mathbf{u}$ and in some cases the leakage power in this direction should be below a threshold. This constraint can be properly added to transceiver designs by judiciously designing $\mathbf{R}_{\mathbf{s}_k}$. This result is very useful for multiuser communications and mutual interference coordination.

A. Linear Transceiver

When the linear transceivers are deployed by the relaying networks as shown in Fig. 1, at the source the transmitted signal satisfies $\mathbf{x}_0 = \mathbf{a}$ and the received signal at the destination is

$$\mathbf{r} = [\prod_{k=1}^{K}\mathbf{H}_k\mathbf{P}_k]\mathbf{a} + \sum_{k=1}^{K-1}\{[\prod_{l=k+1}^{K}\mathbf{H}_l\mathbf{P}_l]\mathbf{n}_k\} + \mathbf{n}_K, \tag{6}$$

where $\prod_{k=1}^{K}\mathbf{Z}_k$ denotes $\mathbf{Z}_K \times \cdots \times \mathbf{Z}_1$. Meanwhile, at the destination a linear equalizer $\mathbf{G}$ is adopted to recover the desired signal and the data detection mean square error (MSE) matrix is derived to be

$$\mathbf{\Phi}_{\mathrm{MSE}}(\mathbf{G}, \{\mathbf{P}_k\}_{k=1}^{K}) = \mathbb{E}\{(\mathbf{G}\mathbf{r} - \mathbf{a})(\mathbf{G}\mathbf{r} - \mathbf{a})^{\mathrm{H}}\}, \tag{7}$$

where the expectation is taken with respect to random data and noises.

B. Decision Feedback Equalizer

When decision feedback equalizer (DFE) is adopted at the destination and linear precoding is used at the source as shown in Fig. 2, the transmitted signal at the source is still $\mathbf{a}$ and the received signal at the destination is the same as (6). While the desired signals are recovered through a DFE and the output signal equals

$$\mathbf{y} = \{\mathbf{G}[\prod_{k=1}^{K}\mathbf{H}_k\mathbf{P}_k] - \mathbf{B}\}\mathbf{a} + \sum_{k=1}^{K-1}\{[\prod_{l=k+1}^{K}\mathbf{H}_l\mathbf{P}_l]\mathbf{n}_k\} + \mathbf{n}_K, \tag{8}$$

where $\mathbf{B}$ is a strictly lower triangular matrix. With DEF the data detection MSE matrix equals

$$\mathbf{\Phi}_{\mathrm{MSE}}(\mathbf{G}, \{\mathbf{P}_k\}_{k=1}^{K}, \mathbf{B}) = \mathbb{E}\{(\mathbf{y} - \mathbf{a})(\mathbf{y} - \mathbf{a})^{\mathrm{H}}\}. \tag{9}$$

C. Tomlinson-Harashima Precoding

On the other hand, according to dirty paper coding (DPC) mutual interference can be precanceled by exploiting Tomlinson-Harashima Precoding (THP) at the source. As shown in Fig. 3, at the transmitter, before sending out the data vector $\mathbf{a}$ is fed into the a precoding unit comprising of a $N \times N$ feedback matrix $\mathbf{B}$ and a nonlinear modulo operator, $\mathrm{MOD}(\bullet)$ [28]. The output signal of THP is equivalent to the following equation [22]

$$\mathbf{x}_0 = (\mathbf{I} + \mathbf{B})^{-1}(\underbrace{\mathbf{a} + \mathbf{d}}_{\triangleq \mathbf{s}}), \tag{10}$$

where the vector $\mathbf{d}$ guarantees $\mathbf{x}_0$ in a finite region and it can be simply removed at receiver by modulo operation [28]. When the elements of $\mathbf{a}$ are independent and identically distributed (i.i.d.) over the constellation and the dimension of modulation constellation is large, $\mathbf{x}_0$ can also be considered as i.i.d. [28], i.e., $\mathbf{R}_{\mathbf{x}_0} = \sigma_s^2 \mathbf{I}_N$. For high dimensional modulation constellations, it also holds that $\sigma_s^2 \approx \sigma_a^2$ irrespective of a scaling factor as the scalar factor is almost equivalent to one [28]. In this case, the received signal at the destination is

$$\mathbf{r} = [\prod_{k=1}^{K} \mathbf{H}_k \mathbf{P}_k]\mathbf{x}_0 + \sum_{k=1}^{K-1} \{[\prod_{l=k+1}^{K} \mathbf{H}_l \mathbf{P}_l]\mathbf{n}_k\} + \mathbf{n}_K. \tag{11}$$

With THP the data detection MSE matrix at the destination is

$$\mathbf{\Phi}_{\mathrm{MSE}}(\mathbf{G}, \{\mathbf{P}_k\}_{k=1}^K, \mathbf{B}) = \mathbb{E}\{(\mathbf{G}\mathbf{r} - \mathbf{s})(\mathbf{G}\mathbf{r} - \mathbf{s})^{\mathrm{H}}\}. \tag{12}$$

With the definition of an auxiliary matrix

$$\mathbf{C} = \mathbf{I} + \mathbf{B} \tag{13}$$

the previous MSE matrices given by (7), (9) and (12) are unified into the following formulation

$$\begin{aligned} &\mathbf{\Phi}_{\mathrm{MSE}}(\mathbf{G}, \{\mathbf{P}_k\}_{k=1}^K, \mathbf{C}) \\ =&\mathbf{G}[\mathbf{H}_K \mathbf{P}_K \mathbf{R}_{\mathbf{x}_{K-1}} \mathbf{P}_K^{\mathrm{H}} \mathbf{H}_K^{\mathrm{H}} + \mathbf{R}_{n_K}]\mathbf{G}^{\mathrm{H}} + \mathbf{C}\mathbf{C}^{\mathrm{H}}\sigma_{\mathbf{a}}^2 - \sigma_{\mathbf{a}}^2 \mathbf{C}[\prod_{k=1}^{K} \mathbf{H}_k \mathbf{P}_k]^{\mathrm{H}} \mathbf{G}^{\mathrm{H}} \\ &- \mathbf{G}[\prod_{k=1}^{K} \mathbf{H}_k \mathbf{P}_k]\mathbf{C}^{\mathrm{H}}\sigma_{\mathbf{a}}^2. \end{aligned} \tag{14}$$

III. Problem Formulation

The considered optimization problem of transceiver designs aims at minimizing a matrix-monotone increasing function of the MSE matrix [23]. For example, regarding linear transceiver designs, a series of performance metrics but not all can be formulated as additively Schur-convex/Schur-concave functions of the diagonal elements of the MSE matrix $\mathbf{\Phi}_{\mathrm{MSE}}(\mathbf{G}, \{\mathbf{P}_k\}_{k=1}^K, \mathbf{C})$, i.e., $\mathbf{d}(\mathbf{\Phi}_{\mathrm{MSE}}(\mathbf{G}, \{\mathbf{P}_k\}_{k=1}^K, \mathbf{C}))$ where symbol $\mathbf{d}(\mathbf{Z})$ denotes a vector consisting of the diagonal elements of $\mathbf{Z}$, i.e., $\mathbf{d}(\mathbf{Z}) = [[\mathbf{Z}]_{1,1}, [\mathbf{Z}]_{2,2}, \cdots, [\mathbf{Z}]_{N,N}]^{\mathrm{T}}$. In the following, we will discuss the considered transceiver designs case by case.

(1) *Weighted MSE*: With the data MSE matrix defined in (14), weighted MSE can be directly written as

$$\text{Obj 1:} \quad \mathrm{Tr}[\mathbf{W}\mathbf{\Phi}_{\mathrm{MSE}}(\mathbf{G}, \{\mathbf{P}_k\}_{k=1}^K, \mathbf{C} = \mathbf{I})] \tag{15}$$

where the weighting matrix $\mathbf{W}$ is a positive semi-definite matrix. This is different from the work in [29] which only restricts to diagonal weighting matrices.

(2) *Capacity*: Capacity maximization is another important and widely used performance metric for transceiver design. The capacity maximization is equivalent to minimize the following objective function

$$\text{Obj 2: } \log|\mathbf{\Phi}_{\mathrm{MSE}}(\mathbf{G}, \{\mathbf{P}_k\}_{k=1}^K, \mathbf{C}=\mathbf{I})|. \tag{16}$$

(3) *Additively Schur-convex*: design. In general, when a certain fairness in the sense of arithmetic mean is required such as worst/MAX MSE minimization, the objective function can be represented as [30]

$$\text{Obj 3: } f_{\mathrm{A-Schur}}^{\mathrm{Convex}}[\mathbf{d}(\mathbf{\Phi}_{\mathrm{MSE}}(\mathbf{G}, \{\mathbf{P}_k\}_{k=1}^K, \mathbf{C}=\mathbf{I}))] \tag{17}$$

where $f_{\mathrm{A-Schur}}^{\mathrm{Convex}}(\bullet)$ is an increasing additively Schur-convex (A-Shur-Convex) function.

(4) *Additively Schur-concave*: When a preference is given to certain data streams (e.g., the data streams with better channel state information are more preferred), the objective function can be written as [30]

$$\text{Obj 4: } f_{\mathrm{A-Schur}}^{\mathrm{Concave}}[\mathbf{d}(\mathbf{\Phi}_{\mathrm{MSE}}(\mathbf{G}, \{\mathbf{P}_k\}_{k=1}^K, \mathbf{C}=\mathbf{I}))] \tag{18}$$

where $f_{\mathrm{A-Schur}}^{\mathrm{Concave}}(\bullet)$ is an increasing additively Schur-concave (A-Schur-Concave) function. For example, weighted MSE minimization with diagonal weighting matrices is a special case of this kind of objective functions.

For nonlinear transceiver designs, a series of performance metrics can be formulated as multiplicatively Schur-convex/Schur-concave functions of the diagonal elements of $\mathbf{\Phi}_{\mathrm{MSE}}(\mathbf{G}, \{\mathbf{P}_k\}_{k=1}^K, \mathbf{C})$.

(5) *Multiplicatively Schur-convex*: With a certain fairness requirement is added on the geometric mean of the transmitted data streams, the objective function can be written as [31]

$$\text{Obj 5: } f_{\mathrm{M-Schur}}^{\mathrm{Convex}}[\mathbf{d}(\mathbf{\Phi}_{\mathrm{MSE}}(\mathbf{G}, \{\mathbf{P}_k\}_{k=1}^K, \mathbf{C}))] \tag{19}$$

where $f_{\mathrm{M-Schur}}^{\mathrm{Convex}}(\bullet)$ is an increasing multiplicatively Schur-concave (M-Schur-Concave) function.

(6) *Multiplicatively Schur-concave*: With THP or DFE structure, when some preference is added to different data stream via using different weighting factors, the objective function can be written as [31]

$$\text{Obj 6: } f_{\mathrm{M-Schur}}^{\mathrm{Concave}}[\mathbf{d}(\mathbf{\Phi}_{\mathrm{MSE}}(\mathbf{G}, \{\mathbf{P}_k\}_{k=1}^K, \mathbf{C}))] \tag{20}$$

where $f_{\mathrm{M-Schur}}^{\mathrm{Concave}}(\bullet)$ is an increasing multiplicatively Schur-concave (M-Schur-Convex) function.

In summary, the optimization problem of transceiver designs can be formulated as follows

$$\begin{aligned} \min_{\mathbf{G},\{,\mathbf{P}_k\},\mathbf{C}} \quad & f\left[\mathbf{\Phi}_{\mathrm{MSE}}(\mathbf{G},\{\mathbf{P}_k\}_{k=1}^K,\mathbf{C})\right] \\ \text{s.t.} \quad & \mathrm{Tr}(\mathbf{P}_k\mathbf{R}_{\mathbf{x}_{k-1}}\mathbf{P}_k^{\mathrm{H}}) \leq P_k \\ & \mathbf{P}_k\mathbf{R}_{\mathbf{x}_{k-1}}\mathbf{P}_k^{\mathrm{H}} \preceq \mathbf{R}_{\mathbf{s}_k} \\ & [\mathbf{C}]_{i,i} = 1 \\ & [\mathbf{C}]_{i,j} = 0 \quad \text{for} \quad i > j \end{aligned} \tag{21}$$

where $f(\bullet)$ is a matrix-monotone increasing function. The final two constraints come from the fact that $\mathbf{B}$ is a strictly lower triangular matrix.

It is obvious that there is no constraint on the equalizer $\mathbf{G}$. Thus for the optimal equalizer we can simply differentiate the trace of (14) with respect to $\mathbf{G}$ and then obtain the linear minimum mean square error (LMMSE) equalizer

$$\mathbf{G}_{\mathrm{LMMSE}} = \sigma_{\mathbf{a}}^2[\prod_{k=1}^K \mathbf{H}_k\mathbf{P}_k]^{\mathrm{H}}[\mathbf{H}_K\mathbf{P}_K\mathbf{R}_{\mathbf{x}_{K-1}}\mathbf{P}_K^{\mathrm{H}}\mathbf{H}_K^{\mathrm{H}} + \mathbf{R}_{n_K}]^{-1}, \tag{22}$$

which has the following property [32]

$$\mathbf{\Phi}_{\mathrm{MSE}}(\mathbf{G}_{\mathrm{LMMSE}},\{\mathbf{P}_k\}_{k=1}^K,\mathbf{C}) \preceq \mathbf{\Phi}_{\mathrm{MSE}}(\mathbf{G},\{\mathbf{P}_k\}_{k=1}^K,\mathbf{C}). \tag{23}$$

Because $f(\bullet)$ is matrix-monotone increasing function, (23) implies that $\mathbf{G}_{\mathrm{LMMSE}}$ minimizes the objective function in (21). Plugging the optimal equalizer of (22) into (14), we directly have

$$\mathbf{\Phi}_{\mathrm{MSE}}(\mathbf{G}_{\mathrm{LMMSE}},\{\mathbf{P}_k\}_{k=1}^K,\mathbf{C}) = \mathbf{C}\mathbf{\Phi}_{\mathrm{LMMSE}}(\{\mathbf{P}_k\}_{k=1}^K)\mathbf{C}^{\mathrm{H}} \tag{24}$$

where the inner term on the righthand side is just the MSE matrix derived for linear transceivers

$$\mathbf{\Phi}_{\mathrm{LMMSE}}(\{\mathbf{P}_k\}_{k=1}^K) = \sigma_{\mathbf{a}}^2\mathbf{I}_N - \sigma_{\mathbf{a}}^2[\prod_{k=1}^K \mathbf{H}_k\mathbf{P}_k]^{\mathrm{H}}[\mathbf{H}_K\mathbf{P}_K\mathbf{R}_{\mathbf{x}_{K-1}}\mathbf{P}_K^{\mathrm{H}}\mathbf{H}_K^{\mathrm{H}} + \mathbf{R}_{n_K}]^{-1}[\prod_{k=1}^K \mathbf{H}_k\mathbf{P}_k]\sigma_{\mathbf{a}}^2. \tag{25}$$

For multi-hop AF MIMO relaying systems, the received signal at the k^{th} relay node depends on the forwarding matrices at all preceding relays, and it makes the power allocations at different

relays couple with each other. In order to simplify the problem substantially, we first define the following new variable in terms of $\mathbf{P}_k$:

$$\mathbf{F}_k \triangleq \mathbf{P}_k \mathbf{R}_{\mathbf{n}_{k-1}}^{1/2} (\underbrace{\mathbf{R}_{\mathbf{n}_{k-1}}^{-1/2} \mathbf{H}_{k-1} \mathbf{F}_{k-1} \mathbf{F}_{k-1}^{\mathrm{H}} \mathbf{H}_{k-1}^{\mathrm{H}} \mathbf{R}_{\mathbf{n}_{k-1}}^{-1/2} + \mathbf{I}}_{\triangleq \mathbf{\Pi}_{k-1}})^{1/2} \mathbf{Q}_k^{\mathrm{H}}, \tag{26}$$

where $\mathbf{Q}_k$ is an unknown unitary matrix. The introduction of $\mathbf{Q}_k$ comes from the fact that for a positive semi-definite matrix $\mathbf{M}$, its square roots generally has the form $\mathbf{M}^{1/2}\mathbf{Q}$ where $\mathbf{Q}$ is a unitary matrix. Note that at the source node $\mathbf{F}_1 = \sigma_{\mathbf{a}} \mathbf{P}_1 \mathbf{Q}_1^{\mathrm{H}}$. Meanwhile, with the new variables $\mathbf{F}_k$, the corresponding transmit covariance matrix at the k^{th} node can be rewritten as

$$\mathbf{P}_k \mathbf{R}_{\mathbf{x}_{k-1}} \mathbf{P}_k^{\mathrm{H}} = \mathbf{F}_k \mathbf{F}_k^{\mathrm{H}} \tag{27}$$

With the new definition in (26), the matrix $\mathbf{\Phi}_{\mathrm{LMMSE}}(\{\mathbf{Q}_k\}, \{\mathbf{F_k}\})$ is transformed to be a more compact formulation

$$\begin{aligned}
&\mathbf{\Phi}_{\mathrm{LMMSE}}(\{\mathbf{Q}_k\}, \{\mathbf{F_k}\}) \\
=&\sigma_{\mathbf{a}}^2 \mathbf{I}_N - \sigma_{\mathbf{a}}^2 [\prod_{k=1}^{K} \mathbf{\Pi}_k^{-1/2} \mathbf{R}_{\mathbf{n}_k}^{-1/2} \bar{\mathbf{H}}_k \mathbf{F}_k \mathbf{Q}_k]^{\mathrm{H}} [\prod_{k=1}^{K} \underbrace{\mathbf{\Pi}_k^{-1/2} \mathbf{R}_{\mathbf{n}_k}^{-1/2} \mathbf{H}_k \mathbf{F}_k}_{\triangleq \boldsymbol{A}_k} \mathbf{Q}_k] \\
=&\sigma_{\mathbf{a}}^2 \mathbf{I}_N - \sigma_{\mathbf{a}}^2 \mathbf{Q}_1^{\mathrm{H}} \boldsymbol{A}_1^{\mathrm{H}} \mathbf{Q}_2^{\mathrm{H}} \cdots \boldsymbol{A}_K^{\mathrm{H}} \boldsymbol{A}_K \cdots \mathbf{Q}_2 \boldsymbol{A}_1 \mathbf{Q}_1.
\end{aligned} \tag{28}$$

It is obvious that with the new variables $\mathbf{F}_k$'s, the constraints become independent with each other. Putting (27) and (28) into the original optimization (21), the transceiver design problem can be reformulated as

$$\begin{aligned}
\min_{\{\mathbf{F}_k\}, \{\mathbf{Q}_k\}, \mathbf{C}} \quad & f\left[\mathbf{C} \mathbf{\Phi}_{\mathrm{LMMSE}}(\{\mathbf{F}_k\}, \{\mathbf{Q}_k\}) \mathbf{C}^{\mathrm{H}}\right] \\
\text{s.t.} \quad & \mathrm{Tr}(\mathbf{F}_k \mathbf{F}_k^{\mathrm{H}}) \leq P_k \\
& \mathbf{F}_k \mathbf{F}_k^{\mathrm{H}} \preceq \mathbf{R}_{\mathbf{s}_k} \\
& [\mathbf{C}]_{i,i} = 1 \\
& [\mathbf{C}]_{i,j} = 0 \quad \text{for} \quad i > j.
\end{aligned} \tag{29}$$

Matrix Version Weighting Operation Interpretation:

If the following analysis, we will simply set $\sigma_{\mathbf{a}}^2 = 1$ without loss of generality. It is worth noting that $\mathbf{I} - \mathbf{Q}_k^{\mathrm{H}} \boldsymbol{A}_k^{\mathrm{H}} \boldsymbol{A}_k \mathbf{Q}_k$ is the data detection MSE matrix for LMMSE estimator in the

$k^{\rm th}$ hop. For LMMSE estimators the estimated signal is independent of the residual noise [32] and then $\mathbf{Q}_k^{\rm H}\boldsymbol{A}_k^{\rm H}\boldsymbol{A}_k\mathbf{Q}_k$ is the covariance matrix of the estimated signal at the $k^{\rm th}$ relay node. Roughly speaking, the singular values $\boldsymbol{A}_k\mathbf{Q}_k$ reflect the strength of the recovered signals.

Just as discussed in [33], AF MIMO relaying can be recognized as a certain matrix version weighting operation. For example, if we only focus the final two hops, it is a standard dual hop AF MIMO relaying system and its MSE matrix can be written in the following form

$$\underbrace{\mathbf{Q}_{K-1}^{\rm H}\boldsymbol{A}_{K-1}^{\rm H}}_{\boldsymbol{W}^{\rm H}}(\mathbf{I}-\mathbf{Q}_K^{\rm H}\boldsymbol{A}_K^{\rm H}\boldsymbol{A}_K\mathbf{Q}_K)\underbrace{\boldsymbol{A}_{K-1}\mathbf{Q}_{K-1}}_{\boldsymbol{W}}+\underbrace{\mathbf{I}-\mathbf{Q}_{K-1}^{\rm H}\boldsymbol{A}_{K-1}^{\rm H}\boldsymbol{A}_{K-1}\mathbf{Q}_{K-1}}_{\boldsymbol{\Pi}}. \tag{30}$$

In accordance to the definition of matrix version weighting in [33], the matrix weighting of the $(K-1)^{\rm th}$ hop on the $K^{\rm th}$ hop is carried out by multiplying a matrix version slope $\boldsymbol{W}$ and adding a matrix version intercept $\boldsymbol{\Pi}$. Notice that the matrix version intercept is just the MSE matrix for the $K-1$ hop. As shown in Fig. 4, repeat this process and finally we will have the exact formula of $\boldsymbol{\Phi}_{\rm LMMSE}(\{\mathbf{F}_k\},\{\mathbf{Q}_k\})$. Interestingly, the roles of THP and DFE also fall into the category of this kind of matrix weighting operations with matrix version slope $\boldsymbol{W}=\mathbf{C}^{\rm H}$ and matrix version intercept $\boldsymbol{\Pi}=\mathbf{0}$. In this case, the matrix version intercept equals zero because THP or DFE does not introduce noises.

IV. Reformulation of the Considered Optimization Problem

In the optimization problem (29) discussed above, there are three kinds of variables, i.e., $\mathbf{C}$, $\mathbf{Q}_k$'s and $\mathbf{F}_k$'s. In this section, we will try our best to simplify the problem (29) by first deriving the optimal solutions of $\mathbf{C}$ and $\mathbf{Q}_k$'s to be the functions of $\mathbf{F}_k$'s and then the number of variables will be significantly reduced.

A. Optimal $\mathbf{C}$

Different from the optimal solution of the equalizer, the optimal solutions of $\mathbf{C}$ are different for linear and nonlinear transceivers. For linear transceivers, $\mathbf{C}$ is a constant identity matrix. On the other hand, for nonlinear transceiver designs with DFE or THP, we have the following result [22]

$$\mathbf{C}_{\rm opt}=\mathrm{diag}\{[\mathbf{L}_{1,1},\cdots,\mathbf{L}_{N,N}]^{\rm T}\}\mathbf{L}^{-1}, \tag{31}$$

based on which at the optimum values the objective functions in Cases 5 and 6 are equivalent to

$$\text{Obj 5: } f_{\mathrm{M-Schur}}^{\mathrm{Convex}}(\mathbf{d}^2[\mathbf{L}]) \quad \text{with} \quad \mathbf{\Phi}_{\mathrm{LMMSE}}(\{\mathbf{F}_k\},\{\mathbf{Q}_k\}) = \mathbf{L}\mathbf{L}^{\mathrm{H}}, \tag{32}$$

$$\text{Obj 6: } f_{\mathrm{M-Schur}}^{\mathrm{Concave}}(\mathbf{d}^2[\mathbf{L}]) \quad \text{with} \quad \mathbf{\Phi}_{\mathrm{LMMSE}}(\{\mathbf{F}_k\},\{\mathbf{Q}_k\}) = \mathbf{L}\mathbf{L}^{\mathrm{H}}. \tag{33}$$

B. Optimal $\mathbf{Q}_k$'s

Defining a unitary matrix $\mathbf{U}_{\mathbf{\Theta}}$ based on the eigenvalue decomposition (EVD) of

$$\boldsymbol{A}_1^{\mathrm{H}}\mathbf{Q}_2^{\mathrm{H}}\boldsymbol{A}_2^{\mathrm{H}}\cdots\boldsymbol{A}_K^{\mathrm{H}}\boldsymbol{A}_K\cdots\boldsymbol{A}_2\mathbf{Q}_2\boldsymbol{A}_1 = \mathbf{U}_{\mathbf{\Theta}}\mathbf{\Lambda}_{\mathbf{\Theta}}\mathbf{U}_{\mathbf{\Theta}}^{\mathrm{H}} \tag{34}$$

with eigenvalues in decreasing order, following the same logic in [22], [23] it can be proved that the optimal $\mathbf{Q}_1$ equals

$$\mathbf{Q}_1 = \mathbf{U}_{\mathbf{\Theta}}\mathbf{U}_{\mathbf{\Omega}}^{\mathrm{H}} \tag{35}$$

in which $\mathbf{U}_{\mathbf{\Omega}}$ has the following solution

$$\mathbf{U}_{\mathbf{\Omega}} = \begin{cases} \mathbf{U}_{\mathbf{W}} & \text{for Obj 1} \\ \mathbf{U}_{\mathrm{Arb}} & \text{for Obj 2} \\ \mathbf{Q}_{\mathrm{DFT}} & \text{for Obj 3} \\ \mathbf{I}_N & \text{for Obj 4} \\ \mathbf{Q}_{\mathbf{T}} & \text{for Obj 5} \\ \mathbf{I}_N & \text{for Obj 6} \end{cases} \tag{36}$$

where $\mathbf{U}_{\mathbf{W}}$ is the unitary matrix of the EVD of $\mathbf{W}$ with eigenvalues in decreasing order and $\mathbf{U}_{\mathrm{Arb}}$ is an arbitrary unitary matrix with property dimension. Moreover, the unitary matrix $\mathbf{Q}_{\mathrm{DFT}}$ is discrete Fourier transform (DFT) matrix and the matrix $\mathbf{Q}_{\mathbf{T}}$ is the unitary matrix which makes the Cholesky factorization matrix of $\mathbf{Q}_1^{\mathrm{H}}(\mathbf{I}-\boldsymbol{A}_1^{\mathrm{H}}\mathbf{Q}_2^{\mathrm{H}}\cdots\boldsymbol{A}_K^{\mathrm{H}}\boldsymbol{A}_K\cdots\mathbf{Q}_2\boldsymbol{A}_1)\mathbf{Q}_1$ have identical diagonal elements. Except $\mathbf{Q}_1$ discussed above, the optimal $\mathbf{Q}_k$'s for $k = 2,\cdots,K$ should satisfy the following property [22], [23]

$$\mathbf{Q}_k = \mathbf{V}_{\boldsymbol{A}_k}\mathbf{U}_{\boldsymbol{A}_{k-1}}^{\mathrm{H}}, \quad k = 2,\cdots,K. \tag{37}$$

where the unitary matrices $\mathbf{U}_{\boldsymbol{A}_k}$ and $\mathbf{V}_{\boldsymbol{A}_k}$ come from the singular value decomposition (SVD) $\boldsymbol{A}_k = \mathbf{U}_{\boldsymbol{A}_k}\mathbf{\Lambda}_{\boldsymbol{A}_k}\mathbf{V}_{\boldsymbol{A}_k}^{\mathrm{H}}$ with $\mathbf{\Lambda}_{\boldsymbol{A}_k} \searrow$.

C. The Reformulated optimization problems

Based on the optimal solutions of $\mathbf{C}$ and $\mathbf{Q}_k$'s listed particularly, the original optimization problem (29) becomes

$$\begin{aligned} \min_{\{\mathbf{F}_k\}} \quad & g\left(\left\{\boldsymbol{\lambda}(\mathbf{F}_k^{\mathrm{H}}\mathbf{H}_k^{\mathrm{H}}\mathbf{R}_{\mathbf{n}_k}^{-1}\mathbf{H}_k\mathbf{F}_k)\right\}_{k=1}^{K}\right) \\ \text{s.t.} \quad & \mathrm{Tr}(\mathbf{F}_k\mathbf{F}_k^{\mathrm{H}}) \leq P_k \\ & \mathbf{F}_k\mathbf{F}_k^{\mathrm{H}} \leq \mathbf{R}_{\mathbf{s}_k} \end{aligned} \tag{38}$$

where $\boldsymbol{\lambda}(\mathbf{Z})$ denotes the vector consisting of eigenvalues, i.e., $\boldsymbol{\lambda}(\mathbf{Z}) = [\lambda_1(\mathbf{Z}), \lambda_2(\mathbf{Z}), \cdots, \lambda_N(\mathbf{Z})]$. Furthermore, it should be highlighted that the objective $g(\bullet)$ is a monotonically decreasing function with respect to the following big column vector

$$[\boldsymbol{\lambda}(\mathbf{F}_1^{\mathrm{H}}\mathbf{H}_1^{\mathrm{H}}\mathbf{R}_{\mathbf{n}_1}^{-1}\mathbf{H}_1\mathbf{F}_1), \cdots, \boldsymbol{\lambda}(\mathbf{F}_K^{\mathrm{H}}\mathbf{H}_K^{\mathrm{H}}\mathbf{R}_{\mathbf{n}_K}^{-1}\mathbf{H}_K\mathbf{F}_K)]^{\mathrm{T}}. \tag{39}$$

Based on this fact, jointly considering all possible objective functions, the unified optimization problem is successfully decomposed into a series of sub-problems given by the following formula

$$\begin{aligned} \max_{\mathbf{F}_k} \quad & \boldsymbol{\lambda}\left(\mathbf{F}_k^{\mathrm{H}}\mathbf{H}_k^{\mathrm{H}}\mathbf{R}_{\mathbf{n}_k}^{-1}\mathbf{H}_k\mathbf{F}_k\right) \\ \text{s.t.} \quad & \mathrm{Tr}(\mathbf{F}_k\mathbf{F}_k^{\mathrm{H}}) \leq P_k \\ & \mathbf{F}_k\mathbf{F}_k^{\mathrm{H}} \preceq \mathbf{R}_{\mathbf{s}_k} \\ & \mathrm{Rank}\{\mathbf{F}_k\mathbf{F}_k^{\mathrm{H}}\} \leq N \end{aligned} \tag{40}$$

where the final rank constraint is added to restrict the spatial region of power allocation in order to save energy. The motivation comes from the fact that from physical meaning the number of eigenchannels used in each hop should not be larger than that of the data streams. In nature, problem (40) is a multi-objective optimization problem. In other words, the optimal solutions of (40) are not unique and our focus is to the find the Pareto optimal set. From the multi-objective optimization theory viewpoint, for any given transceiver design, its optimal solution of $\mathbf{F}_k$ is in the Pareto optimal solution set of (40) [34]. In other words, all the common characteristics of the Pareto optimal solutions of (40) will be inherited by the solutions of its special cases. In the following, we focus on the common properties of the Pareto optimal solution set of (40). Based on (40), it can also be concluded that the original optimization problem has been decomposed

into a series of subproblems with much lower dimension. This structure enables the transceiver designs to be well suited for distributed implementation.

V. Transceiver Designs with Pure Shaping Constraints

In the optimization problem (40), except the rank constraint, there are still two constraints i.e., sum power constraint and shaping constraint. If shaping constraint is stricter than sum power constraint, i.e., $\mathrm{Tr}(\mathbf{R}_{\mathbf{s_s}}) \leq P_k$, the sum power constraint can be removed directly. Therefore, the optimization problem (40) can be written as

$$\begin{aligned} \max \quad & \boldsymbol{\lambda}\left(\mathbf{F}_k^{\mathrm{H}}\mathbf{H}_k^{\mathrm{H}}\mathbf{R}_{\mathbf{n}_k}^{-1}\mathbf{H}_k\mathbf{F}_k\right) \\ \text{s.t.} \quad & \mathbf{F}_k\mathbf{F}_k^{\mathrm{H}} \preceq \mathbf{R}_{\mathbf{s}_k} \\ & \mathrm{Rank}\{\mathbf{F}_k\mathbf{F}_k^{\mathrm{H}}\} \leq N. \end{aligned} \tag{41}$$

It is obvious that the above optimization problem is equivalent to the following one

$$\begin{aligned} \max \quad & \boldsymbol{\lambda}\left(\mathbf{R}_{\mathbf{n}_k}^{-1/2}\mathbf{H}_k\mathbf{F}_k\mathbf{F}_k^{\mathrm{H}}\mathbf{H}_k^{\mathrm{H}}\mathbf{R}_{\mathbf{n}_k}^{-1/2}\right) \\ \text{s.t.} \quad & \mathbf{F}_k\mathbf{F}_k^{\mathrm{H}} \preceq \mathbf{R}_{\mathbf{s}_k} \\ & \mathrm{Rank}\{\mathbf{F}_k\mathbf{F}_k^{\mathrm{H}}\} \leq N. \end{aligned} \tag{42}$$

If the rank constraint is inactive i.e., $\mathrm{Rank}\{\mathbf{R}_{\mathbf{s}_k}\} \leq N$ the optimal $\mathbf{F}_k$ equals

$$\mathbf{F}_{k,\mathrm{opt}} = \mathbf{U}_{\mathbf{R}_{\mathbf{s}_k}}\left[\boldsymbol{\Lambda}_{\mathbf{R}_{\mathbf{s}_k}}^{1/2}\ \mathbf{0}\right]\mathbf{U}_{\mathrm{Arb}}^{\mathrm{H}} \tag{43}$$

where the unitary matrix $\mathbf{U}_{\mathbf{R}_{\mathbf{s}_k}}$ and the diagonal matrix $\boldsymbol{\Lambda}_{\mathbf{R}_{\mathbf{s}_k}}$ are defined based on the EVD $\mathbf{R}_{\mathbf{s}_k} = \mathbf{U}_{\mathbf{R}_{\mathbf{s}_k}}\boldsymbol{\Lambda}_{\mathbf{R}_{\mathbf{s}_k}}\mathbf{U}_{\mathbf{R}_{\mathbf{s}_k}}^{\mathrm{H}}$ with $\boldsymbol{\Lambda}_{\mathbf{R}_{\mathbf{s}_k}} \searrow$. On the other hand, when $\mathrm{Rank}\{\mathbf{R}_{\mathbf{s}_k}\} > N$ the optimization problem becomes a little bit more complicated. Notice that when $\mathbf{A} \preceq \mathbf{B}$ it can be concluded that $\lambda_j(\mathbf{A}) \leq \lambda_j(\mathbf{B})$. In this case, it can be easily proved that at the optimum the eigenvalues of $\mathbf{F}_k\mathbf{F}_k^{\mathrm{H}}$ satisfy

$$\lambda_j(\mathbf{F}_k\mathbf{F}_k^{\mathrm{H}}) = \begin{cases} \lambda_j(\mathbf{R}_{\mathbf{s}_k}) & j = 1:N \\ 0 & \mathrm{Otherwise} \end{cases} \tag{44}$$

based on which the shaping constraint in (42) becomes to be

$$\mathbf{F}_k\mathbf{F}_k^{\mathrm{H}} = [\mathbf{U}_{\mathbf{F}_k}]_{:,1:N}[\boldsymbol{\Lambda}_{\mathbf{F}_k}]_{1:N,1:N}[\boldsymbol{\Lambda}_{\mathbf{F}_k}]_{1:N,1:N}^{\mathrm{T}}[\mathbf{U}_{\mathbf{F}_k}]_{:,1:N}^{\mathrm{H}} \preceq \mathbf{R}_{\mathbf{s}_k} \tag{45}$$

Notice that when $\mathbf{A} \preceq \mathbf{B}$ in general we can only argue that $\lambda_j(\mathbf{A}) \leq \lambda_j(\mathbf{B})$ but we cannot say $\mathbf{A}$ and $\mathbf{B}$ have the same eigenvectors in EVD. Here, as $\lambda_j(\mathbf{F}_k\mathbf{F}_k^{\mathrm{H}}) = \lambda_j(\mathbf{R}_{\mathbf{s}_k})$ for $j = 1:N$, in Appendix A it can be proved that $[\mathbf{U}_{\mathbf{F}_k}]_{:,1:N} = [\mathbf{U}_{\mathbf{R}_{\mathbf{s}_k}}]_{:,1:N}$ and then we have

$$\mathbf{F}_k\mathbf{F}_k^{\mathrm{H}} = [\mathbf{U}_{\mathbf{R}_{\mathbf{s}_k}}]_{:,1:N}[\mathbf{\Lambda}_{\mathbf{R}_{\mathbf{s}_k}}]_{1:N,1:N}[\mathbf{U}_{\mathbf{R}_{\mathbf{s}_k}}]_{:,1:N}^{\mathrm{H}}. \tag{46}$$

It means that the optimal solution of $\mathbf{F}_k$ is

$$\mathbf{F}_{k,\mathrm{opt}} = \mathbf{U}_{\mathbf{R}_{\mathbf{s}_k}} \begin{bmatrix} [\mathbf{\Lambda}_{\mathbf{R}_{\mathbf{s}_k}}]_{1:N,1:N}^{1/2} & \\ & \mathbf{0} \end{bmatrix} \mathbf{U}_{\mathrm{Arb}}^{\mathrm{H}}. \tag{47}$$

Based on the previous discussions, we discover that for the transceiver designs with pure shaping constraint, the closed-form optimal solutions of $\mathbf{F}_k$'s are independent of the objective functions and channel realizations. This conclusion is consistent with its counterpart for point-to-point MIMO systems [24].

VI. Transceiver Designs with Joint Power Constraints

In this section, we take a further step to investigate a more complicated case with joint power constraints. In this case, the original optimization problem (40) has the following special formulation

$$\begin{aligned} \max \quad & \boldsymbol{\lambda}\left(\mathbf{F}_k^{\mathrm{H}}\mathbf{H}_k^{\mathrm{H}}\mathbf{R}_{\mathbf{n}_k}^{-1}\mathbf{H}_k\mathbf{F}_k\right) \\ \text{s.t.} \quad & \mathrm{Tr}(\mathbf{F}_k\mathbf{F}_k^{\mathrm{H}}) \leq P_k \\ & \mathbf{F}_k\mathbf{F}_k^{\mathrm{H}} \leq \tau_{k,\max}\mathbf{I} \\ & \mathrm{Rank}\{\mathbf{F}_k\mathbf{F}_k^{\mathrm{H}}\} \leq N. \end{aligned} \tag{48}$$

It should be highlighted that for joints power constraints, we only focus on the case in which the sum power constraint is always active. It is because if the sum power constraint is inactive, the considered optimization problem will reduce to a special case of that discussed in the previous section. Fortunately, we discover that actually the derived solution is also suitable for the case where the sum power constraint is inactive. The formulation of joint power constraints can be interpreted as an effect way to model transceiver designs peak power constraint [25]. The above

optimization problem (48) is equivalent to the following optimization problem [35]

$$\begin{aligned} \textbf{Prob. 1:} \quad \max \quad & \mathbf{F}_k^{\mathrm{H}}\mathbf{H}_k^{\mathrm{H}}\mathbf{R}_{\mathbf{n}_k}^{-1}\mathbf{H}_k\mathbf{F}_k \\ \text{s.t.} \quad & \mathrm{Tr}(\mathbf{F}_k\mathbf{F}_k^{\mathrm{H}}) \leq P_k \\ & \mathbf{F}_k\mathbf{F}_k^{\mathrm{H}} \leq \tau_{k,\max}\mathbf{I} \\ & \mathrm{Rank}\{\mathbf{F}_k\mathbf{F}_k^{\mathrm{H}}\} \leq N. \end{aligned} \tag{49}$$

It is worth noting that the optimization problem (49) is in nature a multi-objective optimization problem in the field of positive semi-definite matrices [34]. Our attention is still focused on the Pareto optimal solution set. Because of the matrix version objective, directly deriving the Pareto optimal set is challenging. Necessary transformations are needed.

A. The Structures of Optimal Solutions

Defining the Pareto optimal solutions $\mathbf{F}_{k,\mathrm{PO}}$'s for **Prob. 1**, $\mathbf{F}_{k,\mathrm{PO}}$'s must satisfy all the constraints i.e., $\mathrm{Tr}(\mathbf{F}_{k,\mathrm{PO}}\mathbf{F}_{k,\mathrm{PO}}^{\mathrm{H}}) \leq P_k$, $\mathbf{F}_{k,\mathrm{PO}}\mathbf{F}_{k,\mathrm{PO}}^{\mathrm{H}} \leq \tau_{k,\max}\mathbf{I}$ and $\mathrm{Rank}\{\mathbf{F}_{k,\mathrm{PO}}\mathbf{F}_{k,\mathrm{PO}}^{\mathrm{H}}\} \leq N$. Furthermore, for any given Pareto optimal solution $\mathbf{F}_{k,\mathrm{PO}}$, it is impossible to find a feasible $\mathbf{F}_k$ under the constraints specified in **Prob. 1** which satisfies $\mathbf{F}_k^{\mathrm{H}}\mathbf{H}_k^{\mathrm{H}}\mathbf{R}_{\mathbf{n}_k}^{-1}\mathbf{H}_k\mathbf{F}_k \succ \mathbf{F}_{k,\mathrm{PO}}^{\mathrm{H}}\mathbf{H}_k^{\mathrm{H}}\mathbf{R}_{\mathbf{n}_k}^{-1}\mathbf{H}_k\mathbf{F}_{k,\mathrm{PO}}$. The Pareto optimal solution set of $\mathbf{F}_k$ of **Prob. 1** consists of the optimal $\mathbf{F}_k$ of the following optimization problem by traversing all possible $\mathbf{F}_{k,\mathrm{PO}}$

$$\begin{aligned} \textbf{Prob. 2:} \quad \max_{\alpha,\mathbf{F}_k} \quad & \alpha \\ \text{s.t.} \quad & \mathbf{F}_k^{\mathrm{H}}\mathbf{H}_k^{\mathrm{H}}\mathbf{R}_{\mathbf{n}_k}^{-1}\mathbf{H}_k\mathbf{F}_k = \alpha\mathbf{F}_{k,\mathrm{PO}}^{\mathrm{H}}\mathbf{H}_k^{\mathrm{H}}\mathbf{R}_{\mathbf{n}_k}^{-1}\mathbf{H}_k\mathbf{F}_{k,\mathrm{PO}} \\ & \mathrm{Tr}(\mathbf{F}_k\mathbf{F}_k^{\mathrm{H}}) \leq P_k \\ & \mathbf{F}_k\mathbf{F}_k^{\mathrm{H}} \leq \tau_{k,\max}\mathbf{I} \\ & \mathrm{Rank}\{\mathbf{F}_k\mathbf{F}_k^{\mathrm{H}}\} \leq N. \end{aligned} \tag{50}$$

When computing optimal $\mathbf{F}_k$ and α, $\mathbf{F}_{k,\mathrm{PO}}$ is a given matrix instead of an unknown matrix. It is proved in Appendix B regardless of the specific values of $\mathbf{F}_{k,\mathrm{opt}}$ the optimal solution of $\mathbf{F}_k$ of **Prob. 2** always satisfies the following structure

$$\mathbf{F}_{k,\mathrm{opt}} = \mathbf{V}_{\boldsymbol{\mathcal{H}}}\boldsymbol{\Lambda}_{\mathbf{F}_k}\mathbf{U}_{\mathrm{Arb}}^{\mathrm{H}} \quad \text{with} \quad [\boldsymbol{\Lambda}_{\mathbf{F}_k}]_{i,i} \leq \tau_{\max} \tag{51}$$

where the unitary $\mathbf{V}_{\boldsymbol{\mathcal{H}}}$ is defined based SVD $\mathbf{R}_{\mathbf{n}_k}^{-1/2}\mathbf{H}_k = \mathbf{U}_{\boldsymbol{\mathcal{H}}_k}\Lambda_{\boldsymbol{\mathcal{H}}_k}\mathbf{U}_{\boldsymbol{\mathcal{H}}_k}^{\mathrm{H}}$ with $\Lambda_{\boldsymbol{\mathcal{H}}_k} \searrow$. Additionally. the first N diagonal elements of the diagonal matrix $\mathbf{\Lambda}_{\mathbf{F}_k}$ are still unknown variables and the other diagonal elements are all zeros. As the Pareto optimal solution set of $\mathbf{F}_k$ of **Prob. 1** can be achieved by the resulting optimal solution of **Prob. 2** via changing $\mathbf{F}_{k,\mathrm{opt}}$, it can be directly concluded that any Pareto optimal solution of **Prob. 1** satisfies the optimal structure given by (51). Based on the optimal structure the remaining problem becomes how to compute $\mathbf{\Lambda}_{\mathbf{F}_k}$, and it will be discussed in the following section.

B. Cave Water-filling Solutions

At the beginning of this section, we want to highlight that the solutions of $\mathbf{\Lambda}_{\mathbf{F}_k}$ in (51) are determined by the specific formulas of objective function. Different objective functions usually have different optimal $\mathbf{\Lambda}_{\mathbf{F}_k}$. However, the derivation logics for different objective functions are exactly the same, which all exploit the famous Karush-Kuhn-Tucker (KKT) conditions and the final solutions are variants of classic water-filling solutions, which are termed as cave water-filling solutions [36]. In the following two most representative objectives are investigated, i.e., A-Schur-Convex and M-Schur-Convex objective functions. For these objective functions, the optimal solutions are independent of the specific formulations of the objective functions [22], [30], [31], [35]. In terms of BER, these objective functions usually enjoy much better performance over their respective corresponding Schur-concave counterparts [31].

M-Schur-Convex:

Based on the optimal structure given by (51), the transceiver designs with M-Schur-Convex objective functions is equivalent to

$$\begin{aligned} \min_{f_{k,i}^2} \quad & \sum_{i=1}^{N} \log\left(1 - \frac{\prod_{k=1}^{K} f_{k,i}^2 h_{k,i}^2}{\prod_{k=1}^{K}(f_{k,i}^2 h_{k,i}^2 + 1)}\right) \\ \text{s.t.} \quad & \sum_{i=1}^{N} f_{k,i}^2 \leq P_k \\ & f_{k,i}^2 \leq \tau_{k,\max}. \end{aligned} \tag{52}$$

Generally, the considered optimization problem (52) is nonconvex and thus it is difficult to derive the closed-form optimal solutions. Following the logic in [37], an iterative procedure is further

exploited to solve the unknown variables. Defining the following auxiliary variable

$$a_{k,i} = \prod_{l \neq k} \frac{f_{l,i}^2 h_{l,i}^2}{f_{l,i}^2 h_{l,i}^2 + 1} \tag{53}$$

the Lagrangian of (52) is of the following form

$$\begin{aligned}\mathcal{L}(\{f_{k,i}^2\}, \mu_k, \{\gamma_{k,i}\}, \{l_{k,i}\}) =& \sum_{i=1}^{N} \log\left(1 - a_{k,i} \frac{f_{k,i}^2 h_{k,i}^2}{f_{k,i}^2 h_{k,i}^2 + 1}\right) + \mu_k (\sum_{i=1}^{N} f_{k,i}^2 - P_k) \\ &+ \sum_{i=1}^{N} \{\gamma_{k,i}(f_{k,i}^2 - \tau_{k,\max})\} - \sum_{i=1}^{N} l_{k,i} f_{k,i}^2, \end{aligned} \tag{54}$$

where $f_{k,i}^2$'s are taken as the variables and there are hidden constraints that $f_{k,i}^2 \geq 0$. Based on the KKT conditions we have the follow equation

$$\mu_k + \gamma_{k,i} - l_{k,i} = \underbrace{\frac{a_{k,i} h_{k,i}^2}{(1 - a_{k,i})(f_{k,i}^2 h_{k,i}^2 + 1)^2 + a_{k,i}(f_{k,i}^2 h_{k,i}^2 + 1)}}_{\triangleq \hat{\mathcal{H}}_{k,i}(f_{k,i}^2)} \tag{55}$$

based on which $f_{k,i}^2$ can be solved to be

$$f_{k,i}^2 = \begin{cases} \frac{1}{h_{k,i}^2}\left(\frac{-a_{k,i} + \sqrt{a_{k,i}^2 + 4(1-a_{k,i}) a_{k,i} h_{k,i}^2/\mu_k}}{2(1-a_{k,i})} - 1\right)^+ & \mu_k \geq \hat{\mathcal{H}}_{k,i}(\tau_{k,\max}) \\ \tau_{k,\max} & \mu_k < \hat{\mathcal{H}}_{k,i}(\tau_{k,\max}) \end{cases} \tag{56}$$

where the Lagrange multiplier μ_k makes sure $\sum_i f_{k,i}^2 = P_k$. The conditions $\mu_k \geq \hat{\mathcal{H}}_{k,i}(\tau_{k,\max})$ and $\mu_k < \hat{\mathcal{H}}_{k,i}(\tau_{k,\max})$ mean that the power invested on each eigenchannel cannot exceed $\tau_{k,\max}$.

A-Schur-Convex

On the other hand, exploiting the optimal structure in (51) the optimization problem with A-Schur-Convex objective functions is equivalent to the following problem

$$\begin{aligned} \min_{f_{k,i}^2} \quad & \sum_{i=1}^{N} \left(1 - \frac{\prod_{k=1}^{K} f_{k,i}^2 h_{k,i}^2}{\prod_{k=1}^{K}(f_{k,i}^2 h_{k,i}^2 + 1)}\right) \\ \text{s.t.} \quad & \sum_{i=1}^{N} f_{k,i}^2 \leq P_k \\ & f_{k,i}^2 \leq \tau_{k,\max}. \end{aligned} \tag{57}$$

Similarly, the Lagrangian of (57) equals

$$\begin{aligned}\mathcal{L}(\{f_{k,i}^2\}, \mu_k, \{\gamma_{k,i}\}, \{l_{k,i}\}) =& \sum_{i=1}^{N} \left(1 - \frac{\prod_{k=1}^{K} f_{k,i}^2 h_{k,i}^2}{\prod_{k=1}^{K}(f_{k,i}^2 h_{k,i}^2 + 1)}\right) + \mu_k (\sum_{i=1}^{N} f_{k,i}^2 - P_k) \\ &+ \sum_{i} \{\gamma_{k,i}(f_{k,i}^2 - \tau_{k,\max})\} - \sum_{i} l_{k,i} f_{k,i}^2. \end{aligned} \tag{58}$$

Based on its KKT conditions, we will obtain the following equation with respect to $f_{k,i}^2$

$$\mu_k + \gamma_{k,i} - l_{k,i} = \frac{a_{k,i} h_{k,i}^2}{(h_{k,i}^2 f_{k,i}^2 + 1)^2} \triangleq \tilde{\mathcal{H}}_{k,i}(f_{k,i}^2) \tag{59}$$

based on which $f_{k,i}^2$ can be solved to be

$$f_{k,i}^2 = \begin{cases} \left(\sqrt{\frac{a_{k,i}}{\mu_k h_{k,i}^2}} - \frac{1}{h_{k,i}^2} \right)^+ & \mu_k \geq \tilde{\mathcal{H}}_{k,i}(\tau_{k,\max}) \\ \tau_{k,\max} & \mu_k < \tilde{\mathcal{H}}_{k,i}(\tau_{k,\max}) \end{cases} \tag{60}$$

where the Lagrange multiplier μ_k makes sure $\sum_i f_{k,i}^2 = P_k$. Additionally, the conditions $\mu_k \geq \tilde{\mathcal{H}}_{k,i}(\tau_{k,\max})$ and $\mu_k < \tilde{\mathcal{H}}_{k,i}(\tau_{k,\max})$ also mean that the power invested on each eigenchannel cannot be larger than $\tau_{k,\max}$.

Algorithm 1 Cave Water-Filling Algorithm

$\mathcal{C} = \{$Indexes of all the eigenchannels$\}$
Initialize : Take waterfilling of P_k over $\mathcal{C}$ without considering $\tau_{k,\max}$.
while length(find(PowerAllo $> \tau_{k,\max}$)) > 0 **do**
  $\{$Indexmax$\}$ = Indexes of find(PowerAllo $> \tau_{k,\max}$);
  $\{$Indexnormal$\} = \mathcal{C}/\{$posIndex$\}$(exclusion operation);
  Set PowerAllo(Indexmax) $= \tau_{k,\max}$;
  Set $L =$ Cardinality of $\{$Indexmax$\}$;
  Take waterfilling of $P_k - L\tau_{k,\max}$ over $\{$Indexnormal$\}$ without considering $\tau_{k,\max}$.
end while
return PowerAllo

Due to the fact that there are ceiling constraints on each eigenchannel, the previous results can be named as cave water-filling solutions [36]. In order to show clearly how to compute the cave water-filling solutions, a detailed diagram for the implementation of the previous cave water-filling solutions is given in **Algorithm 1**. It is worth noting that **Algorithm 1** is not restricted to the specific formulas of cave water-filling solutions.

Remark: When channel estimation errors are taken into account, we will have $\mathbf{H}_k = \hat{\mathbf{H}}_k + \Delta\mathbf{H}_k$ where $\hat{\mathbf{H}}_k$ is the channel estimation in the k^{th} hop and $\Delta\mathbf{H}_k$ is the corresponding channel estimation error. If the elements of $\Delta\mathbf{H}_k$ are i.i.d random variables with mean zero and variance

$\sigma_{e_k}^2$, our proposed solutions for the transceiver designs under joint power constraints can be directly to extend to the robust case by simply replacing $\mathbf{H}_k$ by $\hat{\mathbf{H}}_k$ and $\sigma_{n_k}^2$ by $\sigma_{n_k}^2 + P_k\sigma_{e_k}^2$.

VII. Simulation Results and Discussions

In this section, the performance of the transceiver designs under covariance shaping constraints will be evaluated by simulations. Without loss of generality, a three-hop AF MIMO relaying networks is simulated, in which there is one source, two relays and one destination. In addition, it is also assumed that all nodes are equipped with 4 antennas. The entries of the channel matrix in each hop are i.i.d. circularly symmetric complex Gaussian distributed with zero mean and unit variance. The source node aims to transmit four independent data streams to the destination. In the following figures, each point is an average of 2000 independent trials. The signal-to-noise ration (SNR) in each hop is defined as $\mathrm{SNR}_k = P_k/\sigma_{n_k}^2$ and for simplicity in our simulations it is set that $P_1 = P_2 = P_3 = 4$ and $\mathrm{SNR}_1 = \mathrm{SNR}_2 = \mathrm{SNR}_3 = \mathrm{SNR}$ (different SNRs are realized by adjusting noise variances).

Firstly, the performance of the transceiver designs with pure shaping constraints is assessed by the simulations. In this case, it is a natural problem how to choose $\mathbf{R}_{\mathbf{s}_k}$'s in shaping constraints. In the existing work [24], the covariance shaping matrices are assumed to be known a priori. Regarding their explicit formulas, only the simplest diagonal structure is given but without any theoretical analysis and simulation to support it. In this simulation we want to model per-antenna power constraints by constructing $\mathbf{R}_{\mathbf{s}_k}$'s, and the diagonal elements of $\mathbf{R}_{\mathbf{s}_k}$ must be equal to or smaller than some prescribed threshold values. In our setting, threshold values are set to be $[0.4\ 0.8\ 1.2\ 1.6]$ without loss of generality. In the following, two detailed schemes are proposed to construct $\mathbf{R}_{\mathbf{s}_k}$'s.

The design of $\mathbf{R}_{\mathbf{s}_k}$ should be much better if it is independent of specific channel realizations. As in nature $\mathbf{R}_{\mathbf{s}_k}$ can be understood as a correlation matrix, the first one is to exploit the well-known exponential structure as follows and denoted by $\mathbf{R}_{\mathbf{s},1}$

$$\mathbf{R}_{\mathbf{s},1} = \mathrm{diag}\{\{\sqrt{p_j}\}_{j=1}^4\} \begin{bmatrix} 1 & \rho & \rho^2 & \rho^3 \\ \rho & 1 & \rho & \rho^2 \\ \rho^2 & \rho & 1 & \rho \\ \rho^3 & \rho^2 & \rho & 1 \end{bmatrix} \mathrm{diag}\{\{\sqrt{p_j}\}_{j=1}^4\} \tag{61}$$

where $0 \leq \rho < 1$ is the exponential factor. The term $\mathrm{diag}\{\{\sqrt{p_j}\}_{j=1}^{4}\}$ aims at making sure the diagonal elements equal to the prescribed thresholds and meanwhile guaranteeing $\mathbf{R}_{\mathbf{s}_k}$ is a Hermitian matrix via simple linear operations.

To make a comparison with the exponential structure another choice is to produce $\mathbf{R}_{\mathbf{s}_k}$ based on the following special structure $\mathbf{R}_{\mathbf{s},2}$ whose eigenvectors are the same as those of the corresponding channel matrix

$$\mathbf{R}_{\mathbf{s},2} = \mathbf{V}_{\boldsymbol{\mathcal{H}}_k} \boldsymbol{\Lambda}_k \mathbf{V}_{\boldsymbol{\mathcal{H}}_k}^{\mathrm{H}}, \tag{62}$$

where the diagonal entries of the diagonal matrix $\boldsymbol{\Lambda}_k$ are adjustable. The produce is in nature to solve a linear equation array, that adjusting $\boldsymbol{\Lambda}_k$ makes the diagonal elements equivalent to the threshold values. Unfortunately, there is a problem. From physical meaning, $\mathbf{R}_{\mathbf{s}_k}$ must be positive semidefinite, however this fact cannot always hold in the computation of $\boldsymbol{\Lambda}_k$. In other words, after computation some diagonal entries of $\boldsymbol{\Lambda}_k$ may be negative. To overcome this problem, here two methods are adopted. One is to simply set the negative diagonal entries to be zeros. The other is to set them to a positive value η instead of zero, which is designed empirically. Followup, these two operations may violate the constraints on the diagonal elements of $\mathbf{R}_{\mathbf{s}_k}$ as they make $\mathbf{R}_{\mathbf{s}_k}$ more positive. As a result, two weighting operations are exploited further to make the constraints satisfied, which are named matrix weighting and scalar weighting, respectively:

$$\textbf{Matrix Weighting :}\ \ \mathbf{R}_{\mathbf{s},2} = \mathrm{diag}\{\{\sqrt{\beta_j}\}_{j=1}^{4}\} \mathbf{V}_{\boldsymbol{\mathcal{H}}_k} \boldsymbol{\Lambda}_k \mathbf{V}_{\boldsymbol{\mathcal{H}}_k}^{\mathrm{H}} \mathrm{diag}\{\{\sqrt{\beta_j}\}_{j=1}^{4}\} \tag{63}$$

$$\textbf{Scalar Weighting:}\ \ \mathbf{R}_{\mathbf{s},2} = \beta \mathbf{V}_{\boldsymbol{\mathcal{H}}_k} \boldsymbol{\Lambda}_k \mathbf{V}_{\boldsymbol{\mathcal{H}}_k}^{\mathrm{H}}, \tag{64}$$

where β is the maximum scalar that makes the constraints on the diagonal elements satisfied.

Based on the previous two schemes, the capacities of the different designs are plotted in Fig. 5 In Fig. 5 we can see an interesting result that the best performance is achieved when choosing $\mathbf{R}_{\mathbf{s},1}$ with $\rho = 0$. In other words, as shown by the simulation results the simplest diagonal structure is the best. As ρ increases, the capacity decreases. The performance for $\mathbf{R}_{\mathbf{s},2}$ with $\eta = 0$ is very poor. This is because it closes some eigenchannels for transceiver designs. On the other hand, in our simulation we changes the values of η and discover that when $\eta = 1$ much better performance can be obtained. Furthermore, referring to $\mathbf{R}_{\mathbf{s},2}$ matrix weighting operation always outputs scalar weighting operation although scalar weighting operation can keep the eigenvectors of $\mathbf{R}_{\mathbf{s},2}$ unchanged. Based on this result, we may argue that whether eigenvectors

of $\mathbf{R}_{\mathbf{s},2}$ match the channel or not is not important. Similar conclusions can also be achieved for sum MSE minimization as depicted in Fig. 6.

When joint power constraints are taken into account, the effects of peak power constraints are first evaluated by simulation results. The BERs of the linear transceiver designs with different objectives are shown in Fig. 7 when QPSK is used as the modulation constellation. Both A-Schur-Convex and A-Schur-Concave objective functions are simulated here, which correspond MAX-MSE minimization and sum-MSE minimization, respectively [31]. It is obvious that the tighter the joint power constraint is the worse performance the designs have. Additionally, the linear transceiver with A-Shur-Convex objective function always has a much better performance in terms of BER than its counterpart with A-Shur-Concave objective function. While for capacity maximization as shown in Fig. 8, the story is a little bit different as in high SNR regime, the designs with different peak power constraints have almost the same performance. It is because for capacity maximization, if the sum power constraint is active, at high SNR the optimal solution is to allocate the power uniformly, which will be independent of the peak power constraints.

Furthermore, when THP or DFE is adopted to improve BER at the cost of high complexity, high order modulation is preferred. Under the joint constraints with $\tau_{k,\max} = 1.4$ the BERs of various transceiver designs are further compared in Fig. 9 when 16-QAM constellation is used. For the curves in Fig. 9, Gray code is adopted to further improve the BER performance. Note that when the objective function is M-Schur-Concave, the THP and DFE structures will both reduce to linear capacity maximization transceiver [22]. From Fig. 9 it can be concluded that with fixed modulation constellation, nonlinear transceivers enjoy better BER performance than linear transceiver designs even with A-Shur-Convex objective function. It can also be discovered that the transceiver design with THP performs better than that with DFE. This is because THP is performed at the transmitter and it can avoid error propagation effects compared with DFE. However DFE is performed at the receiver and the received signals are inevitably corrupted by noises.

VIII. Conclusions

In this paper, the transceiver designs for multi-hop AF MIMO relaying communications were investigated in depth under covariance shaping constraints. Under covariance shaping constraints a framework for transceiver designs was proposed in which various linear and

nonlinear transceiver designs can be cast as a unified optimization problem. Afterward, it was discovered that the operations of AF MIMO relaying, THP and DFE can all be understood as a kind of matrix version weighting operations with different matrix version slopes and matrix version intercepts. For both the linear and nonlinear transceiver designs with various objective functions under pure shaping constraints or joint power constraints, the optimal solutions were derived in closed-form. Based on the derived solutions, it can be concluded that the proposed algorithm is well suited for distributed implementation. Finally, the performance comparisons between different designs were given by numerical results.

APPENDIX A
DERIVATION OF $\mathbf{U}_{\mathbf{F}_k}$

At the beginning for convenience the column vectors of $\mathbf{U}_{\mathbf{F}_k}$ and $\mathbf{U}_{\mathbf{R}_{\mathbf{s}_k}}$ are defined as $\mathbf{u}_{f_k,j}$'s and $\mathbf{u}_{s_k,j}$'s i.e.,

$$\begin{aligned}\mathbf{U}_{\mathbf{F}_k} &= [\mathbf{u}_{f_k,1} \ \cdots \mathbf{u}_{f_k,N} \cdots] \\ \mathbf{U}_{\mathbf{R}_{\mathbf{s}_k}} &= [\mathbf{u}_{s_k,1} \ \cdots \mathbf{u}_{s_k,N} \cdots].\end{aligned} \tag{65}$$

Then in the following, the focus is how to prove $\mathbf{u}_{f_k,j} = \mathbf{u}_{s_k,j}$ for $j = 1, \cdots, N$. As $\mathbf{u}_{f_k,j}$ corresponds to the j^{th} largest eigenvalue of $\mathbf{F}_k\mathbf{F}_k^{\text{H}}$, the following equality holds [38]

$$\begin{aligned}\lambda_1(\mathbf{F}_k\mathbf{F}_k^{\text{H}}) &= \max_{\mathbf{u}^{\text{H}}\mathbf{u}=1} \mathbf{u}^{\text{H}}\mathbf{F}_k\mathbf{F}_k^{\text{H}}\mathbf{u} \\ \mathbf{u}_{f_k,1} &= \text{argumax}_{\mathbf{u}^{\text{H}}\mathbf{u}=1}\{\mathbf{u}^{\text{H}}\mathbf{F}_k\mathbf{F}_k^{\text{H}}\mathbf{u}\}\end{aligned} \tag{66}$$

based on which and together with the fact that $\mathbf{F}_k\mathbf{F}_k^{\text{H}} \preceq \mathbf{R}_{\mathbf{s}_k}$ we will directly have the following inequality

$$\lambda_1(\mathbf{F}_k\mathbf{F}_k^{\text{H}}) = \mathbf{u}_{f_k,1}^{\text{H}}\mathbf{F}_k\mathbf{F}_k^{\text{H}}\mathbf{u}_{f_k,1} \leq \mathbf{u}_{f_k,1}^{\text{H}}\mathbf{R}_{\mathbf{s}_k}\mathbf{u}_{f_k,1}. \tag{67}$$

Note that $\lambda_1(\mathbf{F}_k\mathbf{F}_k^{\text{H}})$ is also the largest the eigenvalue of $\mathbf{R}_{\mathbf{s}_k}$ and then the equality $\lambda_1(\mathbf{F}_k\mathbf{F}_k^{\text{H}}) = \mathbf{u}_{f_k,1}^{\text{H}}\mathbf{R}_{\mathbf{s}_k}\mathbf{u}_{f_k,1}$ must hold. In other words, $\mathbf{u}_{f_k,1}$ is also the eigenvector corresponding the maximum eigenvalue for $\mathbf{R}_{\mathbf{s}_k}$, i.e.,

$$\mathbf{u}_{f_k,1} = \mathbf{u}_{s_k,1}. \tag{68}$$

Taking a further step, the second largest eigenvalue of $\mathbf{F}_k\mathbf{F}_k^{\mathrm{H}}$ satisfies [38]

$$\lambda_2(\mathbf{F}_k\mathbf{F}_k^{\mathrm{H}}) = \max_{\mathbf{u}^{\mathrm{H}}\mathbf{u}=1,\mathbf{u}\perp\mathbf{u}_{f_k,1}} \mathbf{u}^{\mathrm{H}}\mathbf{F}_k\mathbf{F}_k^{\mathrm{H}}\mathbf{u}$$

$$\mathbf{u}_{f_k,2} = \mathrm{argumax}_{\mathbf{u}^{\mathrm{H}}\mathbf{u}=1,\mathbf{u}\perp\mathbf{u}_{f_k,1}}\{\mathbf{u}^{\mathrm{H}}\mathbf{F}_k\mathbf{F}_k^{\mathrm{H}}\mathbf{u}\}. \tag{69}$$

Exploiting the facts that $\mathbf{u}_{f_k,1}$ is the maximum eigenvalues's eigenvector of $\mathbf{u}_{f_k,1}$ and $\mathbf{F}_k\mathbf{F}_k^{\mathrm{H}} \preceq \mathbf{R}_{\mathbf{s}_k}$, we will directly have the following inequality

$$\lambda_2(\mathbf{F}_k\mathbf{F}_k^{\mathrm{H}}) \leq \mathbf{u}_{f_k,2}^{\mathrm{H}}\mathbf{R}_{\mathbf{s}_k}\mathbf{u}_{f_k,2}. \tag{70}$$

It is worth noting that $\lambda_2(\mathbf{F}_k\mathbf{F}_k^{\mathrm{H}})$ is also the second largest eigenvalue of $\mathbf{R}_{\mathbf{s}_k}$. Then together with the fact that $\mathbf{u}_{f_k,2} \perp \mathbf{u}_{f_k,1}$, similarly to the previous logic for $\mathbf{u}_{f_k,1}$ the above equality must hold and therefore $\mathbf{u}_{f_k,2}$ is also the eigenvector corresponding the second largest eigenvalue for $\mathbf{R}_{\mathbf{s}_k}$, i.e.,

$$\mathbf{u}_{f_k,2} = \mathbf{u}_{s_k,2}. \tag{71}$$

Repeating this logic, it can be proved that $\mathbf{u}_{f_k,j} = \mathbf{u}_{s_k,j}$ for $j = 1, \cdots, N$.

APPENDIX B
DERIVATION OF OPTIMAL STRUCTURE OF $\mathbf{F}_k$'S

In this section, the optimal solution of **Prob. 2** will be derived. By removing the last two constraints, **Prob. 2** is relaxed to be the following much simpler one which is of the following form

$$\begin{aligned} \textbf{Prob. 3:} \quad \max_{\alpha,\mathbf{F}_k} \quad & \alpha \\ \text{s.t.} \quad & \mathbf{F}_k^{\mathrm{H}}\mathbf{H}_k^{\mathrm{H}}\mathbf{R}_{\mathbf{n}_k}^{-1}\mathbf{H}_k\mathbf{F}_k = \alpha\mathbf{F}_{k,\mathrm{PO}}^{\mathrm{H}}\mathbf{H}_k^{\mathrm{H}}\mathbf{R}_{\mathbf{n}_k}^{-1}\mathbf{H}_k\mathbf{F}_{k,\mathrm{PO}} \\ & \mathrm{Tr}(\mathbf{F}_k\mathbf{F}_k^{\mathrm{H}}) \leq P_k. \end{aligned} \tag{72}$$

Based on the SVD $\mathbf{R}_{\mathbf{n}_k}^{-1/2}\mathbf{H}_k = \mathbf{U}_{\boldsymbol{\mathcal{H}}_k}\Lambda_{\boldsymbol{\mathcal{H}}_k}\mathbf{U}_{\boldsymbol{\mathcal{H}}_k}^{\mathrm{H}}$ with $\Lambda_{\boldsymbol{\mathcal{H}}_k} \searrow$, it has been shown in Appendix A in [35] that the optimal solutions have the following structure

$$\mathbf{F}_{k,\mathrm{opt}} = \mathbf{V}_{\boldsymbol{\mathcal{H}}}\boldsymbol{\Lambda}_{\mathbf{F}_k}\mathbf{U}_{\mathrm{Arb}}^{\mathrm{H}} \quad \text{with} \quad \boldsymbol{\Lambda}_{\mathbf{F}_k}^{\mathrm{T}}\Lambda_{\boldsymbol{\mathcal{H}}_k}^{\mathrm{T}}\Lambda_{\boldsymbol{\mathcal{H}}_k}\boldsymbol{\Lambda}_{\mathbf{F}_k} \searrow . \tag{73}$$

In the following we will show that the final two constraints in **Prob. 2** will be automatically satisfied.

Because $\mathrm{Rank}\{\mathbf{F}_{k,\mathrm{PO}}\mathbf{F}_{k,\mathrm{PO}}^{\mathrm{H}}\} \leq N$, from the optimal structure in (73) it is obvious that $\mathrm{Rank}\{\mathbf{F}_{k,\mathrm{opt}}\mathbf{F}_{k,\mathrm{opt}}^{\mathrm{H}}\} = \mathrm{Rank}\{\mathbf{F}_{k,\mathrm{PO}}\mathbf{F}_{k,\mathrm{PO}}^{\mathrm{H}}\} \leq N$. Therefore the rank constraints are automatically satisfied. In the following, we will show that the optimal value of α satisfies $\alpha = 1$. If $\alpha < 1$, it is obvious that the computed $\mathbf{F}_k$ is not optimal as we can simply set $\mathbf{F}_k = \mathbf{F}_{k,\mathrm{PO}}$ to achieve a better objective value without violating any constraint. Otherwise if $\alpha > 1$ it contradicts with the fact $\mathbf{F}_{k,\mathrm{PO}}$ is Pareto optimal. In this case, as $\mathbf{F}_k^{\mathrm{H}}\mathbf{H}_k^{\mathrm{H}}\mathbf{R}_{\mathbf{n}_k}^{-1}\mathbf{H}_k\mathbf{F}_k = \alpha\mathbf{F}_{k,\mathrm{PO}}^{\mathrm{H}}\mathbf{H}_k^{\mathrm{H}}\mathbf{R}_{\mathbf{n}_k}^{-1}\mathbf{H}_k\mathbf{F}_{k,\mathrm{PO}}$ for the optimal values of α and $\mathbf{F}_k$, we can have

$$\begin{aligned}\lambda_i(\frac{1}{\alpha}\mathbf{F}_k^{\mathrm{H}}\mathbf{H}_k^{\mathrm{H}}\mathbf{R}_{\mathbf{n}_k}^{-1}\mathbf{H}_k\mathbf{F}_k) &= \lambda_i(\mathbf{F}_{k,\mathrm{PO}}^{\mathrm{H}}\mathbf{H}_k^{\mathrm{H}}\mathbf{R}_{\mathbf{n}_k}^{-1}\mathbf{H}_k\mathbf{F}_{k,\mathrm{PO}}) \\ &= \lambda_i(\mathbf{R}_{\mathbf{n}_k}^{-1/2}\mathbf{H}_k\mathbf{F}_{k,\mathrm{PO}}\mathbf{F}_{k,\mathrm{PO}}^{\mathrm{H}}\mathbf{H}_k^{\mathrm{H}}\mathbf{R}_{\mathbf{n}_k}^{-1/2}) \\ &\leq \tau_{k,\max}\lambda_i(\mathbf{R}_{\mathbf{n}_k}^{-1/2}\mathbf{H}_k\mathbf{H}_k^{\mathrm{H}}\mathbf{R}_{\mathbf{n}_k}^{-1/2}) \end{aligned} \quad (74)$$

where the final inequality comes from the fact that $\mathbf{F}_{k,\mathrm{PO}}\mathbf{F}_{k,\mathrm{PO}}^{\mathrm{H}} \preceq \tau_{k,\max}\mathbf{I}$. Substituting (73) into (74) we can prove that $\lambda_i(\frac{1}{\alpha}\mathbf{F}_k\mathbf{F}_k^{\mathrm{H}}) \leq \tau_{k,\max}$. Note that at the optimum of **Prob. 3**, $\mathrm{Tr}(\mathbf{F}_{k,,\mathrm{opt}}\mathbf{F}_{k,,\mathrm{opt}}^{\mathrm{H}}) = P_k$ [35] and if $\alpha > 1$, we will have a new variable $\frac{1}{\sqrt{\alpha}}\mathbf{F}_{k,\mathrm{opt}}$ which satisfies all the constraints in **Prob. 2** but $\frac{1}{\alpha}\mathrm{Tr}(\mathbf{F}_{k,\mathrm{opt}}\mathbf{F}_{k,\mathrm{opt}}^{\mathrm{H}}) < P_k$. It means some power is not used and we can simply allocate it to the eigenmodels of $\frac{1}{\alpha}\mathbf{F}_{k,\mathrm{opt}}\mathbf{F}_{k,\mathrm{opt}}^{\mathrm{H}}$ whose power is smaller than the threshold. In other words, we can find a new $\mathbf{F}_k$ which satisfies all the constraints in **Prob. 2** makes $\mathbf{F}_k^{\mathrm{H}}\mathbf{H}_k^{\mathrm{H}}\mathbf{R}_{\mathbf{n}_k}^{-1}\mathbf{H}_k\mathbf{F}_k \succeq \mathbf{F}_{k,\mathrm{PO}}^{\mathrm{H}}\mathbf{H}_k^{\mathrm{H}}\mathbf{R}_{\mathbf{n}_k}^{-1}\mathbf{H}_k\mathbf{F}_{k,\mathrm{PO}}$. This conclusion contradicts with the fact $\mathbf{F}_{k,\mathrm{PO}}$ is Pareto optimal. Finally, it can be concluded that $\alpha = 1$. Together with (74) it can be concluded that the relaxation of two constraints is tight and **Prob. 2** and **Prob. 3** have the same optimal solutions. Therefore, (73) is exactly the optimal structure of the optimal solutions to **Prob. 2**. Note that here we only focus on the case that for the Pareto optimal solution set the sum power constraint is always active. If this assumption is relaxed, a case may happen that the extra power cannot be allocated to the eigenmodels of $\frac{1}{\alpha}\mathbf{F}_{k,\mathrm{opt}}\mathbf{F}_{k,\mathrm{opt}}^{\mathrm{H}}$ because of the peak power constraints. However, in this case **Prob. 1** becomes much simpler as it is a special case with pure shaping constraints. We discover that the structures of the Pareto optimal solutions can still be written as (73).

REFERENCES

[1] N. M. Tehrani, M. Uysal, and H. Yanikomeroglu, "Device-to-device communication in 5G cellular networks: changes, solutions, and future directions," *IEEE Commun. Magazine*, vol. 52, no. 5, pp. 86–92, May 2014.

[2] E. Hossain, M. Rasti, H. Tabassum, and A. Abdelnasser,"Evolution toward 5G multi-tier cellular wireless networks: An interference management perspective," *IEEE Wireless Commun.*, vol. 21, no. 3, pp. 118–127, March 2014.

[3] S. Jin, M. R. Mckay, C. Zhong, and K.-K. Wong, "Ergodic capacity analysis of amplify-and-forward MIMO dual-hop systems," *IEEE Trans. Infor. Theory*, vol. 56, no. 5, pp. 2204-2224, May 2010.

[4] Y. Huang, L. Yang, M. Bengtsson, and B. Ottersten, "A limited feedback joint precoding for amplify-and-forward relaying," *IEEE Trans. Signal Process.*, vol. 59, no. 2, pp. 728–738, Fer. 2010.

[5] W. Xu and X. Dong, "Optimized One-Way Relaying Strategy With Outdated CSI Quantization for Spatial Multiplexing," *IEEE Trans. Signal Process.*, vol. 60, no. 8, pp. 4458–4464, Aug. 2012.

[6] D. Schizas, G. B. Giannakis, and Z.-Q. Luo, "Distributed estimation using reduced dimensionality sensor observations," *IEEE Trans. Signal Process.*, vol. 55, no. 8, pp. 4284–4299, Aug. 2007.

[7] O. Munoz-Medina, J. Vidal, and A. Agustin, "Linear transceiver design in nonregenerative relays with channel state information," *IEEE Trans. Signal Process.*, vol. 55, no. 6, pp. 2593–2604, June 2007.

[8] X. Tang and Y. Hua, "Optimal design of non-regenerative MIMO wireless relays," *IEEE Trans. Wireless Commun.*, vol. 6, no. 4, pp. 1398–1407, Apr. 2007.

[9] W. Guan and H. Luo, "Joint MMSE transceiver design in non-regenerative MIMO relay systems," *IEEE Commun. Lett.*, vol. 12, no. 7, pp. 517–519, July 2008.

[10] F.-S. Tseng, W.-R. Wu, and J.-Y. Wu "Joint source/relay precoder design in nonregenerative cooperative systems using an MMSE criterion," *IEEE Trans. Wireless Commun.*, vol. 8, no. 10, pp. 4928–4933, Oct. 2009.

[11] R. Mo and Y. Chew, "Precoder design for non-regenerative MIMO relay systems," *IEEE Trans. Wireless Commun.*, vol. 8, no. 10, pp. 5041–5049, Oct. 2009.

[12] Y. Rong, X. Tang, and Y. Hua, "A unified framework for optimizing linear nonregenerative multicarrier MIMO relay communication systems," *IEEE Trans. Signal Process.*, vol. 57, no. 12, pp. 4837–4851, Dec. 2009.

[13] C. Li, X. Wang, L. Yang, and W.-P. Zhu, "A joint source and relay power allocation scheme for a class of MIMO relay systems," *IEEE Trans. Signal Process.*, vol. 57, no. 12, pp. 4852–4860, Dec. 2009.

[14] L. Sanguinetti, A. A. D'Amico, and Y. Rong, "A tutorial on the optimization of amplify-and-forward MIMO relay systems," *IEEE J. Selected Areas in Commun.*, vol. 30, no. 8, pp. 1331–1346, Sep. 2012.

[15] L. Zhang, Y. Cai, R. C. de Lamare, and M. Zhao, "Robust multibranch TomlinsonCHarashima precoding design in amplify-and-forward MIMO relay systems," *IEEE Trans. Commun.*, vol. 62, no. 10, pp. 3476–4390, Oct. 2014.

[16] H. Shen, J. Wang, W. Xu, Y. Rong and C. Zhao, "A worst-case robust MMSE transceiver design for nonregenerative MIMO relaying," *IEEE Trans. Wireless Commun.* vo. 12, no. 3, pp/ 695–709, Feb. 2014.

[17] C. Xing, S. Ma, Y.-C. Wu, and T.-S. Ng, "Transceiver design for dual-hop non-regenerative MIMO-OFDM relay systems under channel uncertainties," *IEEE Trans. Signal Process.*, vol. 58, no. 12, pp. 6325–6339, Dec. 2010.

[18] B. K. Chalise and L. Vandendorpe, "Joint linear processing for an amplify-and-forward MIMO relay channel with imperfect channel state information," *EURASIP J. Advances Signal Process.*, vol. 2010, Article ID 640186, 13 pages.

[19] C. Xing, S. Ma, and Y.-C. Wu, "Robust joint design of linear relay precoder and destination equalizer for dual-hop amplify-and-forward MIMO relay Systems," *IEEE Trans. Signal Process.*, vol. 58, no. 4, pp. 2273–2283, Apr. 2010.

[20] Y. Rong, "Robust design for linear non-regenerative MIMO relays with imperfect channel state information," *IEEE Trans. Signal Process.*, vol. 59, no. 5, pp. 2455–2460, May 2011.

[21] Y. Rong and Y. Hua, "Optimality of diagonalization of multi-hop MIMO relays," *IEEE Trans. Wireless Commun.*, vol. 8, pp. 6068-6077, Dec. 2009.

[22] C. Xing, M. Xia, F. Gao and Y.-C. Wu, "Robust transceiver with Tomlinson-Harashima precoding for amplify-and-forward MIMO relaying systems," *IEEE J. Selected Areas in Commun.*, vol. 30, no. 8, pp. 1370–1382, Sep. 2012.

[23] C. Xing, S. Ma, Z. Fei, Y.-C. Wu, and H. Vincent Poor "A general robust linear transceiver design for amplify-and-forward multi-Hop MIMO relaying systems," *IEEE Trans. Signal Process.*, vol. 61, no. 5 pp.1196–1209, Mar. 2013.

[24] D. P. Palomar, "Unified framework for linear MIMO transceivers with Shaping constraints," *IEEE Communi. Lett.*, vol. 8, no. 12, pp. 697–699, Dec. 2004.

[25] J. Dai, C. Chang, W. Xu, and Z. Ye, "Linear precoder optimization for MIMO systems with joint power constraints," *IEEE Trans. Commun.* vol. 60, no. 8, pp. 2240–2254, Aug. 2012.

[26] A. Scaglione, P. Stoica, S. Bardarossa, G. B. Giannakis, and H. Sampath, "Optimal designs for space-time linear precoders and decoders," *IEEE Trans. Signal Proces.*, vol. 50, no. 5, pp. 1051–1064, May 2002.

[27] A. Feiten, R. Mathar, and S. Hanly, "Eigenvalue-based optimum-power allocation for Gaussian vector channels,"*IEEE Trans. Infor. Theory*, vol, 53, no. 6 pp.1939–1943, June 2007.

[28] R. F. H. Fischer, *Precoding and Signal Shaping for Digital Transmission*. New York: Wiley-IEEE, July 2002.

[29] H. Sampath, P. Stoica, and A. Paulraj, "Generalized linear precoder and decoder design for MIMO channels using the weighted MMSE criterion," *IEEE Trans. Commun.*, vol. 49, no. 12, pp. 2198–2206, Dec. 2001.

[30] D. P. Palomar, J. M. Cioffi, and M. A. Lagunas, "Joint Tx-Rx beamforming design for multicarrier MIMO channels: A unified framework for convex optimization," *IEEE Trans. on Signal Process.*, vol. 51, no. 9, pp. 2381–2401, Sep. 2003.

[31] D. P. Palomar and Y. Jiang, *MIMO Transciever Designs via Majorization Theory*, Now Publisher, 2007.

[32] S. Kay, *Fundamental of Statistical Signal Processing: Estimation Theory*, Englewood Cliffs, NJ: Prentice-Hall, 1993.

[33] C. Xing, W. Li, S. Ma, Z. Fei and J. Kuang, "A matrix-field weighted mean-square-error model for MIMO transceiver design," *IEEE Commun. Lett.*, vol. 17, no. 8, pp. 1652–1655, August 2013.

[34] S. Boyd and L. Vandenberghe, *Convex Optimization*. Cambridge University Press. 2004.

[35] C. Xing, S. Ma, and Y. Zhou, "Matrix monotonic optimization for MIMO systems," *to Appear IEEE Trans. Signal Process., available at: http://arxiv.org/abs/1312.1766*

[36] F. Gao, T. Cui, and A. Nallanathan, "Optimal training design for channel estimation in decode-and-forward relay networks with individual and total power constraints," *IEEE Trans. Signal Process.*, vol. 56, no. 12, pp. 5937–5949, Dec. 2008.

[37] W. Yu, W. Rhee, S. Boyd, and J. Cioffi, "Iterative water-filling for Gaussian vector multiple access channels," *IEEE Trans. Infor. Theory*, vol. 50, no. 1, pp.145–151, Jan. 2004.

[38] R. A. Horn and C. R. Johnson, *Matrix Analysis*. Cambridge University Press, 1985.

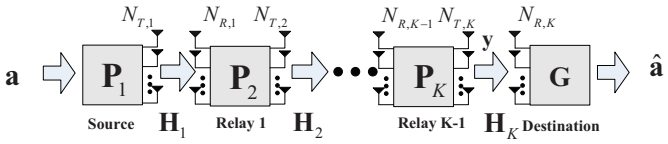

Fig. 1. A multi-hop MIMO relaying system with linear transceivers.

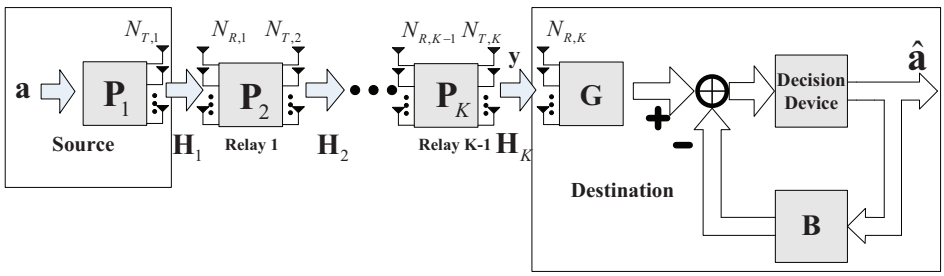

Fig. 2. A multi-hop MIMO relaying system with DFE at destination.

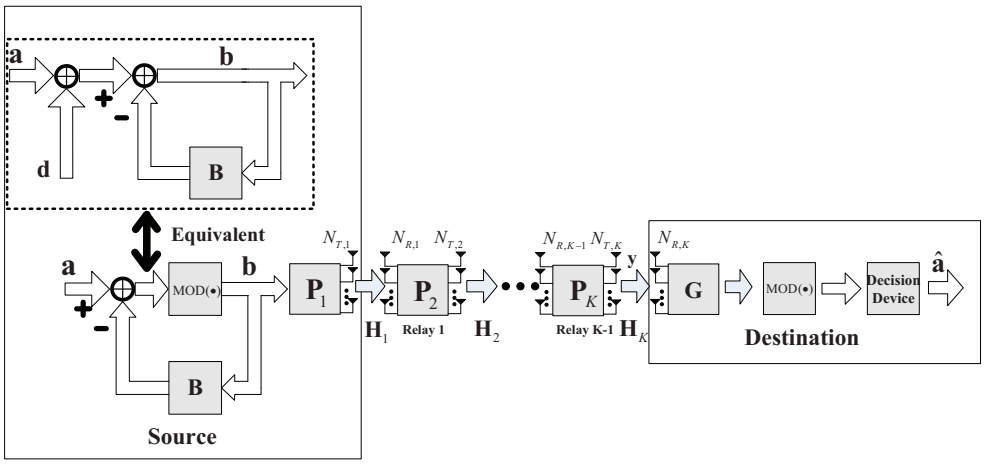

Fig. 3. A multi-hop MIMO relaying system with THP at source.

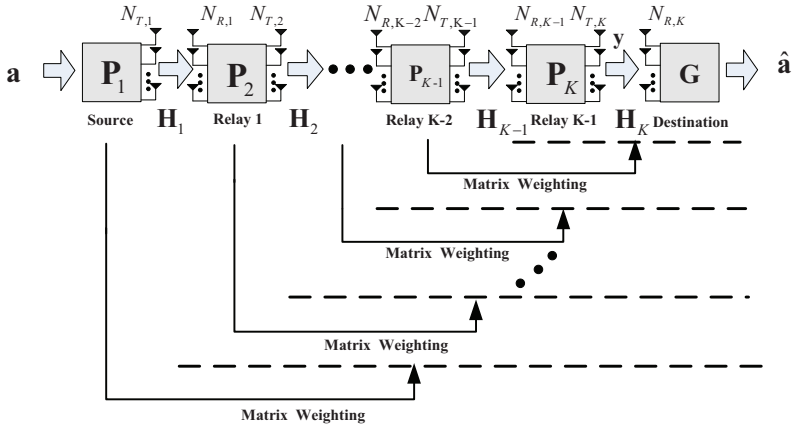

Fig. 4. The understanding of multi-hop AF MIMO relaying from the viewpoint of matrix weighting version operations.

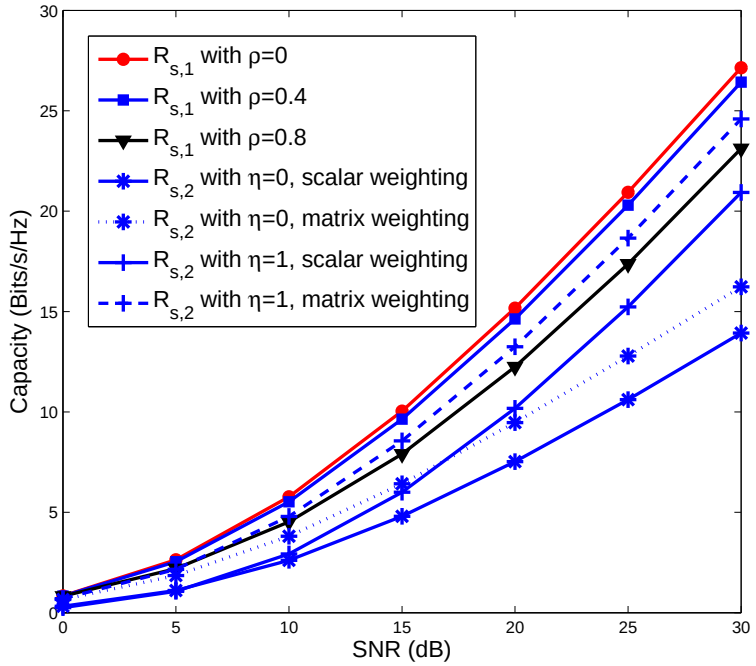

Fig. 5. The channel capacities under various shaping constraints

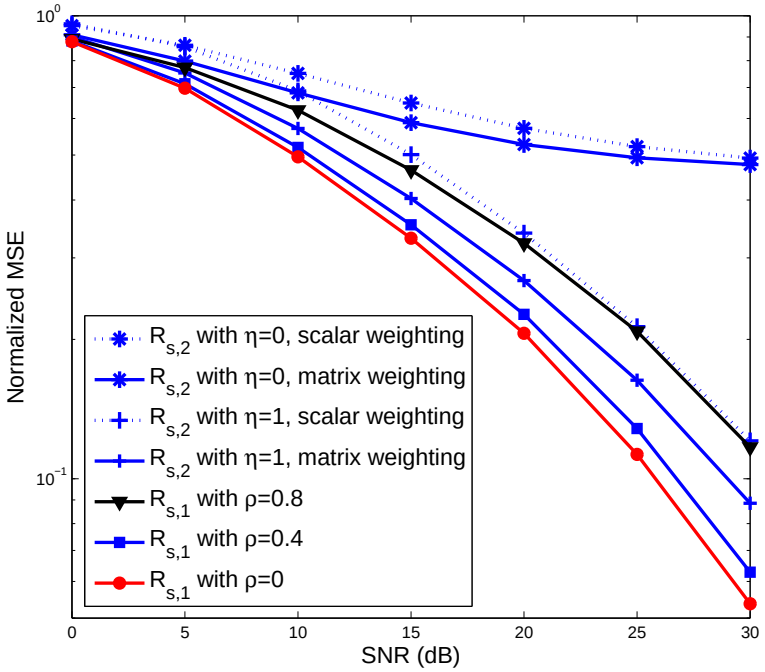

Fig. 6. The normalized MSEs under various shaping constraints

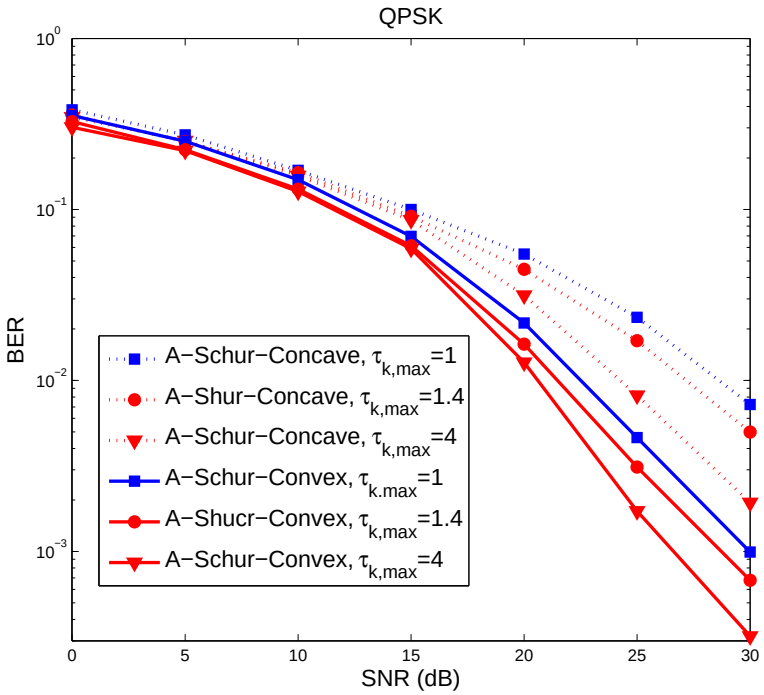

Fig. 7. The BSEs of linear transceiver designs with A-Shur-Convex and A-Shur-Concave objectives for different $\tau_{k,\max}$.

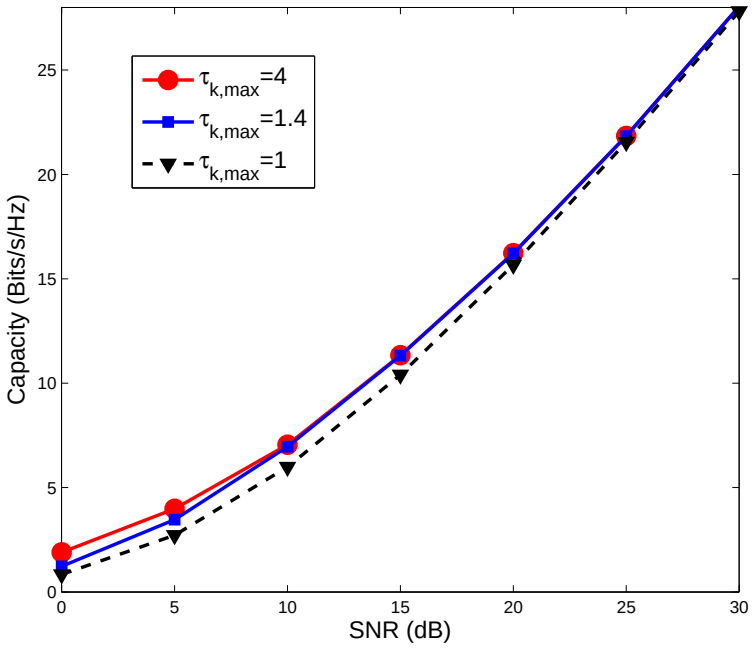

Fig. 8. The channel capacities under different peak power constraints.

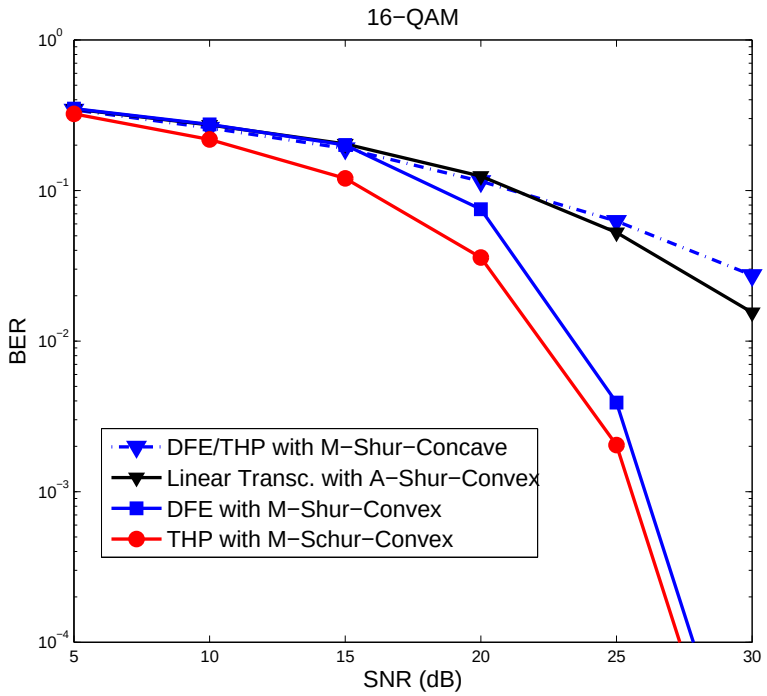

Fig. 9. The BERs of the nonlinear transceiver designs under joint power constraints with $\tau_{k,\max}$=1.4.